Verapamil-sensitive transport of quinacrine and methylene blue via mutant PfCRT reduces the malaria parasite's susceptibility to these tricyclic drugs

Donelly A. van Schalkwyk[1,a,b], Megan N. Nash[1,a], Sarah H. Shafik[1,a], Robert L. Summers[1], Adele M. Lehane[1], Peter J. Smith[2], and Rowena E. Martin[1]*

[1]Research School of Biology, Australian National University, Canberra, ACT, 2601, Australia

[2]Division of Pharmacology, Department of Medicine, University of Cape Town, Private Bag, Rondebosch, 7701, South Africa

[a]D. A. vS., M. N. N., and S. H. S. contributed equally to this work.

[b]Present affiliation/address: Department of Immunology and Infection, Faculty of Infectious and Tropical Diseases, London School of Hygiene and Tropical Medicine, United Kingdom (D. A. vS.).

*Correspondence: Rowena Martin, Research School of Biology, Australian National University, Canberra, ACT, 2601, Australia (rowena.martin@anu.edu.au).

Running title: Transport of tricyclic drugs via PfCRT

Abstract: 200 words

Main text: 3493 words

Title: 150 characters and spaces

Running title: 38 characters and spaces

References: 50

Footnote Page

4)

*Correspondence: Rowena Martin, Research School of Biology, Australian National University, Canberra, ACT, 2601, Australia (rowena.martin@anu.edu.au). Telephone: +61 2 6197 0051; Fax: +61 2 6125 0313.

5)

[b]Present affiliation/address: Department of Immunology and Infection, Faculty of Infectious and Tropical Diseases, London School of Hygiene and Tropical Medicine, United Kingdom (D. A. vS.).

1 **ABSTRACT**

2 ***Background.*** It is becoming increasingly apparent that certain mutations in the *Plasmodium*

3 *falciparum* 'chloroquine resistance transporter' (PfCRT) alter the parasite's susceptibility to

4 diverse compounds. Here we investigated the interaction of PfCRT with three tricyclic

5 compounds that have been used to treat malaria (quinacrine (QC) and methylene blue (MB))

6 or to study *P. falciparum* (acridine orange; AO).

7 ***Methods.*** We measured the antiplasmodial activities of QC, MB, and AO against chloroquine-

8 resistant and chloroquine-sensitive *P. falciparum*, and determined whether QC and AO affect

9 the accumulation and activity of chloroquine in these parasites. We also assessed the ability of

10 mutant (PfCRT[Dd2]) and wild-type (PfCRT[D10]) variants of the protein to transport QC, MB, and

11 AO when expressed at the surface of *Xenopus laevis* oocytes.

12 ***Results.*** Chloroquine-resistance conferring isoforms of PfCRT reduced the sensitivity of the

13 parasite to QC, MB, and AO. In chloroquine-resistant (but not chloroquine-sensitive) parasites,

14 AO and QC increased the parasite's accumulation of, and susceptibility to, chloroquine. All

15 three compounds were shown to bind to PfCRT[Dd2], and the transport of QC and MB via this

16 protein was saturable and inhibited by the chloroquine 'resistance-reverser' verapamil.

17 ***Conclusions.*** Our findings reveal that the PfCRT[Dd2]-mediated transport of tricyclic

18 antimalarials reduces the parasite's susceptibility to these drugs.

19

20 ***Keywords.*** Drug resistance; *Plasmodium falciparum;* tricyclic drug; methylene blue; PfCRT;

21 fluorescent uptake assay; *Xenopus* oocytes.

22

INTRODUCTION

The global campaign to control and eliminate malaria is under serious threat from the emergence and spread of *Plasmodium falciparum* parasites that are resistant to the existing antimalarial drugs [1]. The *P. falciparum* chloroquine resistance transporter (PfCRT) plays a significant role in the phenomenon of drug resistance; mutations in this protein confer resistance to the former 'wonder drug' chloroquine (CQ) and also affect the parasite's susceptibility to a diverse range of molecules, including many of the drugs that have been – or are currently – deployed as antimalarials [e.g., [2] and reviewed in [3]].

PfCRT is located at the membrane of the parasite's digestive vacuole (DV) [4, 5]. Many quinoline-related drugs, including CQ and quinine, accumulate within this acidic compartment (pH 5-5.5) via 'weak-base trapping' [6]. Here they exert an antimalarial effect by preventing the conversion of toxic heme monomers, arising from the parasite's digestion of host hemoglobin, into the inert crystal hemozoin [7, 8]. Resistance to CQ and quinine is associated with a reduction in the accumulation of these drugs in the DV, and several biochemical studies produced indirect evidence for this being attributable to the efflux of CQ and quinine via mutant PfCRT [9-12]. A direct demonstration of this activity was achieved when the wild-type PfCRT (PfCRT[D10]) and a resistance-conferring isoform of the protein (PfCRT[Dd2]) were expressed in *Xenopus laevis* oocytes; PfCRT[Dd2] was shown to possess significant CQ and quinine transport activity, whereas PfCRT[D10] did not [13-15]. These findings aside, much remains to be understood about the protein's ability to recognize and transport diverse compounds.

Here we investigated interactions of PfCRT with quinacrine (QC), methylene blue (MB), and acridine orange (AO). All three molecules contain a tricyclic scaffold (Supplementary Figure 1) and will sequester within the DV due to weak-base trapping or, in the case of the

48   cationic MB, via weak-base trapping and/or oxidation of the reduced forms of the drug [16-

49   19].

50   AO has been employed as a fluorescent dye for the diagnosis of malaria [20] and as a

51   probe for estimating the pH of the DV (pH_{DV}) in CQ-sensitive and CQ-resistant parasites [21-

52   23]. The latter studies reported that CQ-resistant strains have a lower pH_{DV} than their CQ-

53   sensitive counterparts (pH 5.21 versus pH 5.64), and that this could account for the

54   differential accumulation of, and susceptibility to, CQ between these parasites. Alternatively, it

55   has been suggested that the observed difference in the accumulation of AO may instead be

56   due to its export from the DV via mutant PfCRT [24].

57   MB was the first synthetic antimalarial drug and QC, which was derived from MB, was

58   the first synthetic antimalarial to be widely used. Both drugs are thought to inhibit heme

59   detoxification [17, 18, 25], with the redox-cycling capacity of MB potentially exerting an

60   additional parasiticidal effect [18, 26]. Although QC was set aside following the introduction of

61   CQ, structural derivatives of QC have since been deployed (pyronaridine) or are undergoing

62   development [27, 28] as antimalarials. Interest in MB, which until recently was a largely

63   overlooked antimalarial, has been greatly revived by studies that have found it to be (1) a

64   potent gametocytocidal and transmission-blocking agent [29, 30], (2) a potential partner drug

65   that improves the clinical efficacy of amodiaquine and artesunate-amodiaquine [31, 32], and

66   (3) a relatively well-tolerated drug [31-33].

67   A number of in vitro studies have observed cross-resistance between QC and CQ [34-

68   36] and these observations, along with the finding that QC increases the accumulation of CQ in

69   CQ-resistant but not CQ-sensitive parasites [37], implicate mutations in PfCRT as a

70   determinant of the parasite's susceptibility to QC. The relationship between CQ and MB

71   susceptibility in CQ-resistant *P. falciparum* is considerably less clear. Several studies have

72   reported that CQ resistance (and specifically mutant PfCRT) does not impart cross-resistance

73   to MB [38-40], whereas others have observed modest but significant positive correlations

74   between the half-maximal inhibitory concentrations (IC_{50}s) of CQ and MB in *P. falciparum* [17,

75   41, 42].

76   We have sought to elucidate the mechanisms underpinning these observations by

77   ascertaining the nature and strength of the interactions between PfCRT and QC, MB, and AO.

78   Our findings reveal that CQ resistance-conferring isoforms of PfCRT reduce the parasite's

79   susceptibility to tricyclic compounds and that, at least in the cases of QC and MB, this

80   phenomenon is due to the ability of mutant PfCRT to transport these drugs away from their

81   main site of action.

82

83   **MATERIALS AND METHODS**

84

85   **Culture of *P. falciparum*-infected Erythrocytes**

86   The use of human blood in this study was approved by the Australian National University's

87   Human Research Ethics Committee. Two CQ-sensitive strains (D10 and 3D7), three CQ-

88   resistant strains (K1, RSA11, and Dd2), and three *pfcrt* transfectant lines (C2^{GC03}, C4^{Dd2}, and

89   C6^{7G8}; [43]) were cultured and synchronized as described previously [12].

90

91   ***P. falciparum* Drug Susceptibility and Drug Accumulation**

92   Measurements of parasite proliferation, and of [^{3}H]CQ and [^{3}H]AO in accumulation in

93   trophozoite-infected erythrocytes, were performed according to the protocols provided in the

94   Supplementary Materials.

95

96   **Drug Transport in *Xenopus* Oocytes Expressing PfCRT**

97   Oocytes were harvested and prepared using the method described in detail in the

98   Supplementary Materials. PfCRT^{Dd2} and PfCRT^{D10} were expressed at the oocyte plasma

99   membrane using an approach outlined elsewhere [13]. The uptake into oocytes of [^{3}H]CQ, as

100   well as that of unlabelled QC, MB, and AO (all of which fluoresce), was measured using the

101   protocols described in the Supplementary Materials.

102

103   **Statistics**

104   Statistical comparisons were made using the Student's *t*-test for paired or unpaired samples,

105   or ANOVA in conjunction with Tukey's multiple comparisons test.

106

107   **RESULTS**

108

109   **Mutant Forms of PfCRT Decrease the Susceptibility of *P. falciparum* to QC, MB, and AO**

110   The antiplasmodial activities of QC, MB and AO were evaluated in vitro against erythrocytes

111   infected with field-derived CQ-sensitive (D10 or 3D7) or CQ-resistant (RSA11, K1, or Dd2) *P.*

112   *falciparum* strains. The D10 and 3D7 strains carry the wild-type version of PfCRT (PfCRT^{D10}),

113   K1 and Dd2 parasites carry resistance-conferring isoforms of the protein (PfCRT^{K1} and

114   PfCRT^{Dd2}, respectively), and the PfCRT haplotype carried by RSA11 is currently unknown. CQ

115   was included as a reference drug and the resulting IC$_{50}$s are presented in Table 1. QC and MB

116   displayed potent antiplasmodial activities, with IC$_{50}$s against 3D7 parasites of approximately

117   10 and 2.5 nM, respectively. However, these values increased 1.6 to 2-fold when the drugs

118   were tested against the Dd2 strain. AO was the least active of the test compounds, with IC$_{50}$s

119   of ~300 nM against the D10 and 3D7 strains, and these values also increased 1.9 to 2.3-fold in

120   the CQ-resistant strains. The role of PfCRT in the observed decrease in the sensitivities of the

121   CQ-resistant strains to QC, MB, and AO was investigated using a set of isogenic transfectant

122   lines [43], which express the wild-type *pfcrt* allele (C2^{GC03}) or a mutant *pfcrt* allele from either

123   Dd2 (C4^{Dd2}) or the CQ-resistant strain 7G8 (C6^{7G8}). Consistent with what was observed for the

124   field-derived strains, the IC$_{50}$s determined for QC, MB, AO, and CQ were higher in the CQ-

125   resistant lines (C4^{Dd2} and C6^{7G8}) than in the CQ-sensitive C2^{GC03} line (Table 1). CQ-resistant

126   parasites can be partially re-sensitised to CQ in vitro by verapamil (VP) or chlorpheniramine

127   (CP) ([44] and Table 1) – a phenomenon we have shown to be attributable to the ability of

128   these drugs to inhibit CQ transport via mutant PfCRT [13, 14, 45]. In the data presented in

129   Table 1, the presence of 1 μM VP decreased the QC and MB IC$_{50}$s in all of the CQ-resistant

130   strains and lines, and was without effect in their drug-sensitive counterparts. Taken together,

131   these findings suggested that the decreased sensitivity of CQ-resistant parasites to QC and MB

132   was due to the interaction of these drugs with mutant isoforms of PfCRT.

133   VP did not have a significant effect on the activity of AO in any of the parasite types

134   (Table 1). We therefore explored the interaction between AO and PfCRT further by testing

135   whether AO, like VP or CP, potentiates the activity of CQ against CQ-resistant parasites. An

136   initial experiment revealed that the presence of 250 nM AO or 1 μM VP decreased the CQ IC$_{50}$

137   in the K1 strain by ~30% and 65%, respectively, whereas no significant change was observed

138   in the 3D7 strain (Supplementary Table 1). Isobolograms describing the interactions of CQ

139   with AO, and of VP with AO, against the C2^{GCO3} and C4^{Dd2} lines indicated these combinations

140   are additive in C2^{GCO3} parasites, whereas interactions suggestive of synergism were observed

141   in the C4^{Dd2} line (Figure 1). These results suggested that the antiplasmodial activity of

142   combinations of AO with CQ or VP is dependent on the *pfcrt* allele expressed and that AO may

143   behave as a reverser of CQ resistance.

144

145   **QC and AO Increase [³H]CQ Accumulation in CQ-resistant Parasites**

146   The resistance-reversing activity of VP causes an increase in the accumulation of [³H]CQ in

147   CQ-resistant strains, with no such change occurring in drug-sensitive parasites [44]. To

148   investigate whether AO enhances the effects of CQ via the same mechanism, [³H]CQ

149   accumulation was measured in CQ-sensitive and CQ-resistant parasites in the presence or

150   absence of AO, QC, and VP. We found that AO and QC increased the accumulation of [³H]CQ in

151   CQ-resistant parasites when present at 100 nM and 1 μM, respectively (Figure 2). By contrast,

152   1 μM AO had no effect on [3H]CQ accumulation in the drug-sensitive parasites, whereas 100

153   nM QC caused a modest decrease in [3H]CQ accumulation. The latter result suggests that QC

154   reduces the amount of free heme, and therefore CQ-binding sites, within the DV of drug-

155   sensitive parasites, whereas the observed increase in [3H]CQ accumulation in the resistant

156   line indicates that QC possesses a degree of resistance-reversing activity. Moreover, the

157   finding that 1 μM AO and 5 μM VP increased the accumulation of [3H]CQ in the C4[Dd2] line to

158   similar extents (Figure 2*D*) further supported the hypothesis that AO potentiates the activity

159   of CQ against CQ-resistant parasites by blocking the PfCRT-mediated efflux of CQ from the DV.

160

161   **QC, MB, and AO Inhibit the Transport of [3H]CQ via PfCRT[Dd2]**

162   Direct measurements of the abilities of QC, MB, and AO to block CQ transport via PfCRT[Dd2]

163   were undertaken using the *Xenopus* oocyte system. In a preliminary assay in which the

164   tricyclic compounds were each tested at 500 μM, QC and AO caused pronounced reductions in

165   the PfCRT[Dd2]-mediated transport of CQ, whereas MB caused a modest level of inhibition

166   (Figure 3*A*). An analysis of the concentration-dependence of inhibition yielded IC$_{50}$s of 13.5 $\pm$

167   0.9 μM, 41.0 $\pm$ 5.1 μM, and 1.3 $\pm$ 0.2 mM for QC, AO, and MB, respectively (Figures 3*B-D*).

168

169   **QC and MB are Substrates of PfCRT[Dd2]**

170   We further investigated the nature of the interactions of PfCRT[Dd2] with QC, MB, and AO by

171   performing direct measurements of transport in the *Xenopus* oocyte system. We achieved this

172   by re-purposing the radioisotope influx assay for the detection of fluorescent substrates (see

173   Supplementary Materials). In all cases, there was a linear relationship between concentration

174   and fluorescence intensity for QC, MB, and AO (Supplementary Figure 2). It was therefore

175   possible to use the native fluorescence of these compounds to measure their uptake into

176   oocytes expressing different forms of PfCRT.

177   Oocytes expressing PfCRT^{Dd2} were found to accumulate significantly more QC and MB

178   than either non-injected oocytes or oocytes expressing PfCRT^{D10}, consistent with PfCRT^{Dd2},

179   but not PfCRT^{D10}, mediating the transport of these tricyclic drugs (Figures 4*A* and 5*A*; *P*<0.001

180   at 60 minutes). The uptake of QC and MB via PfCRT^{Dd2} was linear over time for at least 2 hours

181   (Figures 4*B* and 5*B*) and the estimated rates of PfCRT^{Dd2}-mediated transport (in picomoles

182   hour^{-1} per oocyte) were 7.01 ± 1.34 (QC) and 4.73 ± 0.14 (MB). An analysis of the

183   concentration-dependence of QC and MB uptake revealed, in both cases, that the component

184   of transport attributable to PfCRT^{Dd2} was saturable (Figures 4*C* and 5*C*). A least squares fit of

185   the Michaelis-Menten equation to the data (Figures 4*D* and 5*D*) yielded apparent Michaelis

186   constants (K_m) of 9.8 ± 1.1 and 123 ± 11.5 μM and maximal velocities (V_{max}) of 16.3 ± 0.7 and

187   202 ± 5 picomoles hour^{-1} per oocyte for QC and MB, respectively. By comparison, in non-

188   injected oocytes and those expressing PfCRT^{D10}, the rate of QC and MB influx increased in a

189   roughly linear manner with increasing concentrations of the drug (Figures 4*C* and 5*C*). This

190   finding, together with the observation that these two oocyte types took up QC or MB to

191   similarly low levels, indicates that this component of accumulation is due to the simple

192   diffusion of the uncharged drug into the oocyte.

193   Several known inhibitors of PfCRT^{Dd2} were tested for their effect on QC and MB uptake

194   in oocytes expressing PfCRT^{D10} or PfCRT^{Dd2}, including VP (250 μM), CQ (750 μM), neurotensin

195   fragment 8-13 (NT; 250 μM) and, in the case of MB uptake, saquinavir (SQV; 250 μM) – which

196   is the most potent of the inhibitors tested [46]. None of the test compounds affected the

197   accumulation of QC or MB in the PfCRT^{D10}-expressing oocytes (Figures 4*E* and 5*E*). By

198   contrast, VP reduced the PfCRT^{Dd2}-mediated uptake of QC and MB by 86 ± 1.6 and 65 ± 4

199   percent, respectively, and SQV caused a 71 ± 3 percent decrease in the transport of MB via

200   PfCRT^{Dd2} (Figures 4*F* and 5*F*). Compared with VP, CQ and NT were less potent inhibitors of QC

201   transport (71 ± 3 and 48 ± 4 percent decreases, respectively) and caused only modest

202   reductions in the PfCRT^{Dd2}-mediated uptake of MB (30 ± 5 and 33 ± 2 percent decreases,

203   respectively).

204   Attempts to detect the transport of AO (75 or 150 μM) via PfCRT were performed at pH

205   4.5, 5.0, 5.5, and 6.0, and a second series of experiments also made measurements of [³H]AO

206   transport over the same pH range. Although several of the assays conducted at pH 5.0

207   appeared to detect a small increase in AO accumulation in the PfCRT[Dd2]-expressing oocytes,

208   the signal was not reproduced in the majority of the assays carried out. This suggested that

209   AO is either not a substrate of PfCRT[Dd2] or that the protein has a very low capacity for AO

210   transport, such that – at least in the oocyte system – it is obscured by the rate of uptake via

211   simple diffusion of the uncharged species (the proportion of AO in the uncharged form is

212   relatively high, even at pH 5.0; Supplementary Table 2). The first scenario raised the

213   possibility that PfCRT[Dd2] (and PfCRT[7G8]) decreases the parasite's susceptibility to AO without

214   mediating the efflux of AO from the DV. We therefore compared the accumulation of [³H]AO

215   between the C2[GC03], C4[Dd2], and C6[7G8] lines and found there to be a modest but significant

216   decrease in [³H]AO accumulation in the CQ-resistant lines (Figure 6). Consistent with the

217   observed failure of VP to increase the activity of AO against CQ-resistant parasites, VP did not

218   produce a PfCRT-dependent increase in the accumulation of [³H]AO (data not shown) and

219   assays performed with the CQ resistance-reverser CP suggest it may, if anything, cause a small

220   decrease in [³H]AO accumulation in the CQ-resistant lines (Supplementary Figure 3).

221

222   **DISCUSSION**

223

224   PfCRT is a significant player in the malaria parasite's steadily expanding resistance to

225   antimalarial drugs, yet relatively little is understood about the extent of its substrate-

226   specificity or the pharmacology of its transport activity. In this study, assays conducted with

227   isogenic transfectant lines, which differ only in the isoform of PfCRT they express, revealed

228   that CQ resistance-conferring isoforms of PfCRT confer a VP-sensitive decrease in the

229 parasite's susceptibility to the tricyclic drugs QC and MB. Characterization of the interaction

230 of these drugs with a mutant isoform of PfCRT (PfCRT[Dd2]) in the *Xenopus* oocyte system

231 provided a mechanistic explanation for this phenomenon; PfCRT[Dd2] can efflux QC and MB out

232 of the parasite's DV and VP inhibits this transport activity. Our findings are also consistent

233 with QC and MB exerting their main schizontocidal activity within the DV, where they are

234 thought to prevent the detoxification of heme and where MB is also likely to disrupt vital

235 redox processes.

236   We also found that parasites carrying a mutant isoform of PfCRT accumulated less of

237 the pH probe AO, and were more resistant to its antiplasmodial activity, than parasites

238 carrying the wild-type version of PfCRT – but these phenomena were not affected by VP. AO

239 did, however, behave as a CQ resistance-reverser; it inhibited CQ transport via PfCRT[Dd2] in the

240 oocyte system (IC$_{50}$ of 41 μM) and chemosensitized CQ-resistant parasites to CQ. The simplest

241 explanation for these observations is that AO binds to mutant PfCRT and is translocated at a

242 low rate, such that it is not consistently detected above the simple diffusion of uncharged AO

243 into the oocyte. These findings render AO unsuitable for comparing the pH$_{DV}$ between CQ-

244 sensitive and CQ-resistant parasites, since the efflux of the probe via mutant PfCRT will result

245 in non-pH-dependent changes in the accumulation of AO. Indeed, no significant difference was

246 observed between CQ-sensitive and CQ-resistant parasites when the pH$_{DV}$ was measured with

247 several other pH-sensitive dyes [24].

248   Our characterization of the interactions between mutant PfCRT and QC in the oocyte

249 system revealed QC transport via PfCRT[Dd2] to be a high-affinity and low-capacity process (e.g.,

250 K$_m$(QC) of 9.8 μM compared with K$_m$(CQ) of 232-245 μM [13, 15]) and QC to be a strong

251 inhibitor of the PfCRT[Dd2]-mediated transport of CQ (QC is comparable in potency to SQV; IC$_{50}$s

252 of 13.5 and 13 μM [46], respectively). These data, which indicate that QC can outcompete CQ

253 for transport via PfCRT[Dd2], provide a mechanistic explanation for the ability of QC to increase

254 [3H]CQ accumulation in CQ-resistant parasites.

255   The finding that the parasite's sensitivity to MB is reduced by the PfCRT-mediated

256   resistance mechanism is consistent with several studies in which a significant correlation

257   between MB and CQ susceptibilities was observed in *P. falciparum* [17, 41, 42], but is at odds

258   with reports of there being no such relationship [38-40]. The basis for this difference is not

259   clear, but may relate to differences in the parasite proliferation protocols between labs. For

260   example, even when the same parasite strains were studied (CQ-sensitive 'D6' and CQ-

261   resistant 'W2'), one group observed modest but significant cross-resistance between CQ and

262   MB [17] whereas another did not [39]. We found PfCRT^{Dd2} to be a medium-affinity and very

263   high-capacity transporter of MB (e.g., the V_{max} values (in picomoles hour^{-1} per oocyte) for MB

264   and CQ are 202 and 61-67 [13, 15], respectively), which may explain, at least in part, why VP

265   and CP inhibited MB uptake to a much lesser extent than what was observed for QC uptake.

266   However, it is also worth noting that MB was a very poor inhibitor of CQ uptake (IC_{50} of 1.3

267   mM) and vice versa. We recently provided evidence for there being at least two distinct, but

268   antagonistically-interacting, substrate-binding sites within PfCRT^{Dd2} and proposed this region

269   of the transporter most likely resembles a cavity with multiple points for substrate

270   interaction [14]. Hence, the relatively poor ability of MB and CQ to interfere with each other's

271   transport could arise from these two drugs binding to largely different sets of attachment

272   points. Likewise, the inability of VP to decrease the AO IC_{50} (and of CP to increase [^{3}H]AO

273   accumulation) in CQ-resistant parasites may be due to there being little or no overlap

274   between the attachment points occupied by AO and VP (or CP).

275   The high-capacity transport of MB via mutant PfCRT, and the resulting reduction in the

276   parasite's susceptibility to the drug, could have future clinical relevance given the potential of

277   MB to serve as a potent transmission-blocking agent and its inclusion in two candidate

278   combination therapies (artesunate-amodiaquine-MB and amodiaquine-MB). It is conceivable

279   that parasites carrying mutant isoforms of PfCRT will be selected by MB-containing

280   treatments, forming a population from which high-level resistance could evolve. Whether this

281   transpires will depend on a number of parameters (none of which are currently known), such

282   as the approximate concentration of MB within the DV and the extent to which it can be

283   lowered by mutant PfCRT, how this fluctuates during the treatment course, and for what

284   period the level of MB within the DV falls beneath the minimum parasiticidal concentration.

285   Moreover, these factors are likely to be affected by the co-administration of MB with

286   amodiaquine, since the latter is suspected to be a substrate of mutant PfCRT [12, 47]. It is also

287   possible that the gametocytocidal activity of MB could be affected by the PfCRT-mediated

288   resistance mechanism; although mature gametocytes no longer digest hemoglobin, they

289   retain both PfCRT as well as vesicles that could be the remnant of, or replacement for, the DV

290   [48, 49].

291   The data presented here have (1) broadened the known substrate range of mutant

292   PfCRT to include tricyclic compounds and (2) established that the PfCRT-mediated efflux of

293   QC and MB from the DV decreases the parasite's sensitivity to these molecules. When taken

294   together with previous studies [13-15], these results reveal a shared mechanism of resistance

295   for CQ, quinine, quinidine, QC, and MB. Our work therefore adds further support to the

296   proposal that PfCRT behaves as a 'multidrug resistance carrier' [3, 50] and highlights the

297   potential for there being an interaction between mutant PfCRT and existing and upcoming

298   antimalarials with quinoline- and acridine-related structures (e.g., ferroquine and

299   pyronaridine).

300   **FIGURE LEGENDS**

301

302   **Figure 1.** Isobolograms describing the interactions of verapamil (VP) with chloroquine (CQ),

303   acridine orange (AO) with CQ, and VP with AO, against erythrocytes infected with C2^{GCO3} or

304   C4^{Dd2} parasites. The data represent the mean ± SEM from 3 independent experiments

305   (performed on different days), within which measurements were averaged from 3 replicates.

306   Where not shown, error bars fall within the symbols. In general, a fractional inhibitory

307   concentration (FIC) of 1.0 suggests that the effects of the two compounds are additive, a FIC ≤

308   0.5 suggests synergism, and a FIC ≥ 4.0 indicates antagonism. The mean FICs for the C2^{GCO3}

309   line were as follows: VP and CQ combination, 1.04; AO and CQ combination, 1.00; VP and AO

310   combination, 0.99. None of these FICs appeared different from 1.0, consistent with all three

311   drug combinations being additive in the CQ-sensitive parasite line. The mean FICs for the

312   C4^{Dd2} line were as follows: VP and CQ combination, 0.54; AO and CQ combination, 0.94; VP

313   and AO combination, 0.84. In all three cases, the mean FICs were below 1.0, but were also

314   above the accepted threshold for categorizing an interaction as synergistic. This finding

315   suggests that the drug combinations were slightly synergistic in the CQ-resistant parasite line.

316

317   **Figure 2.** Effects of quinacrine (QC), acridine orange (AO), and verapamil (VP) on the

318   accumulation of radiolabelled chloroquine ([^{3}H]CQ) by erythrocytes infected with mature

319   trophozoite-stage parasites. Panels *A*, *B*, and *C* show data for CQ-sensitive parasites (C2^{GCO3},

320   D10, and 3D7, respectively). Panels *D*, *E*, and *F* show data for CQ-resistant parasites (C4^{Dd2},

321   RSA11, and K1, respectively). CQ accumulation is expressed in terms of the fold difference in

322   the [^{3}H]CQ 'distribution ratio', which corresponds to the concentration of [^{3}H]CQ within the

323   infected cells relative to the concentration in the extracellular medium. In panels *A* and *D*, the

324   data represent the mean + SEM from 6 independent experiments (performed on different

325   days), within which measurements were averaged from 3 replicates. Panels *B*, *C*, *E*, and *F*

326 show the mean + range/2 of 2 independent experiments (performed on different days),

327 within which measurements were averaged from 3 replicates. In panel E, the SEM for the 100

328 nM AO treatment was very small and the error bar is therefore not visible. The asterisks

329 denote a significant difference in [^{3}H]CQ accumulation between the control treatment and

330 that measured in the presence of QC, AO, or VP: *, $P < 0.05$; **, $P < 0.01$; ***, $P < 0.001$

331 (ANOVA).

332

333 **Figure 3.** Quinacrine (QC), acridine orange (AO), and methylene blue (MB) inhibit the

334 transport of radiolabelled chloroquine ([^{3}H]CQ) via the *Plasmodium falciparum* chloroquine

335 resistance transporter (PfCRT) in *Xenopus laevis* oocytes. A, [^{3}H]CQ uptake into oocytes

336 expressing the Dd2 isoform of PfCRT (PfCRT^{Dd2}; black bars) or the D10 isoform of PfCRT

337 (PfCRT^{D10}; white bars) in the presence of 500 μM unlabelled CQ, QC, AO, or MB. B -D,

338 Concentration-dependent inhibition of the uptake of [^{3}H]CQ into oocytes expressing PfCRT^{Dd2}

339 (black circles) or PfCRT^{D10} (white circles) by QC, AO, or MB. In all panels, [^{3}H]CQ uptake is

340 expressed relative to that measured in the PfCRT^{Dd2}-expressing oocytes under control

341 conditions. The data represent the mean ± SEM from 3 to 5 independent experiments

342 (performed on different days and using oocytes from different frogs), within which

343 measurements were made from 10 oocytes per treatment. Where not shown, error bars fall

344 within the symbols. Note that non-injected oocytes and oocytes expressing PfCRT^{D10} take up

345 [^{3}H]CQ to similar (low) levels via simple diffusion of the neutral species; this represents the

346 "background" level of CQ accumulation in oocytes. In panel A, the asterisks denote a

347 significant difference in [^{3}H]CQ uptake between the control PfCRT^{Dd2} treatment and that

348 measured in the presence of CQ, QC, AO, or MB: ***, $P < 0.001$ (ANOVA). Abbreviation: IC$_{50}$,

349 half-maximal inhibitory concentration.

350

351 **Figure 4.** Quinacrine (QC) transport properties of the *Plasmodium falciparum* chloroquine

352   resistance transporter (PfCRT) in *Xenopus laevis* oocytes. *A*, Oocytes expressing the Dd2

353   isoform of PfCRT (PfCRT^{Dd2}; black circles) showed a marked increase in QC accumulation

354   relative to non-injected oocytes (black triangles) and to those expressing the D10 isoform of

355   PfCRT (PfCRT^{D10}; white circles). Rates of QC uptake (picomoles hour^{-1} per oocyte; $n = 3 \pm$

356   SEM, estimated from uptake at 60 minutes) were as follows: non-injected, 1.74 ± 0.37;

357   PfCRT^{D10}, 1.50 ± 0.20; PfCRT^{Dd2}, 8.62 ± 1.58. *B*, The PfCRT^{Dd2}-mediated uptake of QC

358   (obtained by subtracting the average of the uptake measured in non-injected and PfCRT^{D10}-

359   expressing oocytes from that measured in PfCRT^{Dd2}-expressing oocytes) was approximately

360   linear with time for at least 2 hours. The rate of QC transport via PfCRT^{Dd2}, estimated from

361   uptake at 60 minutes, was 7.01 ± 1.34 picomoles hour^{-1} per oocyte ($n = 3 \pm$ SEM). *C*, The

362   effect of QC concentration on QC uptake by non-injected oocytes (black triangles) and oocytes

363   expressing PfCRT^{D10} (white circles) or PfCRT^{Dd2} (black circles). The accumulation of QC by the

364   control oocytes increased linearly with increasing concentrations of QC, although a second

365   component – attributable perhaps to the binding of QC to the oocyte surface – may have been

366   present below 2.5 μM. *D*, The concentration-dependence of the PfCRT^{Dd2}-mediated transport

367   of QC (in picomoles hour^{-1} per oocyte). *E*, Uptake of QC into oocytes expressing PfCRT^{D10}

368   (white bars) or PfCRT^{Dd2} (black bars) in the presence of 750 μM chloroquine (CQ), 250 μM

369   verapamil (VP), or 250 μM neurotensin (NT). *F*, Inhibition of the PfCRT^{Dd2}-mediated

370   transport of QC by VP, CQ, or NT. The extracellular concentration of QC was 40 μM (panels A

371   and B), 2.5-40 μM (panels C and D), or 10 μM (panels E and F). In all panels except *D*, QC

372   uptake is expressed relative to that measured in the relevant PfCRT^{Dd2} control. The data

373   represent the mean ± SEM from 3 to 11 independent experiments (performed on different

374   days and using oocytes from different frogs), within which measurements were made from 12

375   oocytes per treatment. Where not shown, error bars fall within the symbols. In panels *E* and *F*,

376   the asterisks denote a significant difference in QC uptake between the control PfCRT^{Dd2}

377   treatment and that measured in the presence of VP, CQ, or NT: ***, $P < 0.001$ (ANOVA).

379

380   **Figure 5.** Methylene blue (MB) transport properties of the *Plasmodium falciparum*

381   chloroquine resistance transporter (PfCRT) in *Xenopus laevis* oocytes. *A*, Oocytes expressing

382   the Dd2 isoform of PfCRT (PfCRT[Dd2]; black circles) showed a marked increase in MB

383   accumulation relative to non-injected oocytes (black triangles) and to those expressing the

384   D10 isoform of PfCRT (PfCRT[D10]; white circles). Rates of MB uptake (picomoles hour^{-1} per

385   oocyte; *n* = 3 ± SEM, estimated from uptake at 60 minutes) were as follows: non-injected, 1.61

386   ± 0.07; PfCRT[D10], 1.59 ± 0.08; PfCRT[Dd2], 6.33 ± 0.22. *B*, The PfCRT[Dd2]-mediated uptake of MB

387   (obtained by subtracting the average of the uptake measured in non-injected and PfCRT[D10]-

388   expressing oocytes from that measured in PfCRT[Dd2]-expressing oocytes) was approximately

389   linear with time for at least 2 hours. The rate of MB transport via PfCRT[Dd2], estimated from

390   uptake at 60 minutes, was 4.73 ± 0.14 picomoles hour^{-1} per oocyte (*n* = 3 ± SEM). *C*, The

391   effect of MB concentration on MB uptake by non-injected oocytes (black triangles) and

392   oocytes expressing PfCRT[D10] (white circles) or PfCRT[Dd2] (black circles). The accumulation of

393   MB by the control oocytes increased linearly with increasing concentrations of MB between

394   150 μM and 2 mM MB. A second component was observed below 150 μM; this probably

395   reflects the binding of MB to the oocyte surface. *D*, The concentration-dependence of the

396   PfCRT[Dd2]-mediated transport of MB (in picomoles hour^{-1} per oocyte). *E*, Uptake of MB into

397   oocytes expressing PfCRT[D10] (white bars) or PfCRT[Dd2] (black bars) in the presence of 250 μM

398   saquinavir (SQV), 750 μM chloroquine (CQ), 250 μM verapamil (VP), or 250 μM neurotensin

399   (NT). *F*, Inhibition of the PfCRT[Dd2]-mediated transport of MB by SQV, VP, CQ, or NT. The

400   extracellular concentration of MB was 75 μM (panels A, B, E and F) or 0.025-2 mM (panels C

401   and D). In all panels except *D*, MB uptake is expressed relative to that measured in the

402   relevant PfCRT[Dd2] control. The data represent the mean ± SEM from 3 to 5 independent

403   experiments (performed on different days and using oocytes from different frogs), within

404 which measurements were made from 12 oocytes per treatment. Where not shown, error

405 bars fall within the symbols. In panels *E* and *F*, the asterisks denote a significant difference in

406 MB uptake between the control PfCRT^{Dd2} treatment and that measured in the presence of

407 SQV, VP, CQ, or NT: **, $P < 0.01$; ***, $P < 0.001$ (ANOVA). Abbreviations: K_m, apparent

408 Michaelis constant; V_{max}, maximum velocity.

409

410 **Figure 6.** Accumulation of radiolabelled chloroquine ([^{3}H]CQ) or radiolabelled acridine

411 orange ([^{3}H]AO) by erythrocytes infected with mature trophozoite-stage parasites. The white,

412 black, and gray bars show data for the C2^{GCO3}, C4^{Dd2}, and C6^{7G8} parasite lines, respectively. The

413 accumulation of [^{3}H]drug was expressed as a 'distribution ratio' (i.e., the concentration of

414 [^{3}H]drug within the infected cells relative to the concentration in the extracellular medium)

415 and is shown relative to the ratio measured in the C2^{GCO3} parasites. Under control conditions,

416 the distribution ratios for CQ and AO in the C2^{GCO3} line were 773 ± 95 and 299 ± 31,

417 respectively. The data represent the mean + SEM of 4 independent experiments (performed

418 on different days), within which measurements were averaged from 2 replicates. The

419 asterisks denote a significant difference in [^{3}H]drug accumulation between the C2^{GCO3} line and

420 that measured in the C4^{Dd2} or C6^{7G8} lines: *, $P < 0.05$; **, $P < 0.01$; ***, $P < 0.001$ (ANOVA, with

421 "experiment" nominated as a "blocking factor").

422

427

428 **References**

429

430   1.   Ashley, E.A., M. Dhorda, R.M. Fairhurst, et al. Spread of artemisinin resistance in

431   *Plasmodium falciparum* malaria. N Engl J Med **2014**; 371:411-23.

432   2.   Yuan, J., K.C. Cheng, R.L. Johnson, et al. Chemical genomic profiling for antimalarial

433   therapies, response signatures, and molecular targets. Science **2011**; 333:724-9.

434   3.   Summers, R.L., M.N. Nash, R.E. Martin. Know your enemy: understanding the role of

435   PfCRT in drug resistance could lead to new antimalarial tactics. Cell Mol Life Sci **2012**;

436   69:1967-95.

437   4.   Fidock, D.A., T. Nomura, A.K. Talley, et al. Mutations in the *P. falciparum* digestive

438   vacuole transmembrane protein PfCRT and evidence for their role in chloroquine

439   resistance. Mol Cell **2000**; 6:861-71.

440   5.   Cooper, R.A., M.T. Ferdig, X.Z. Su, et al. Alternative mutations at position 76 of the

441   vacuolar transmembrane protein PfCRT are associated with chloroquine resistance

442   and unique stereospecific quinine and quinidine responses in *Plasmodium falciparum*.

443   Mol Pharmacol **2002**; 61:35-42.

444   6.   Bray, P.G., M. Mungthin, I.M. Hastings, et al. PfCRT and the trans-vacuolar proton

445   electrochemical gradient: regulating the access of chloroquine to ferriprotoporphyrin

446   IX. Mol Microbiol **2006**; 62:238-51.

447   7.   Mungthin, M., P.G. Bray, R.G. Ridley, S.A. Ward. Central role of hemoglobin degradation

448   in mechanisms of action of 4-aminoquinolines, quinoline methanols, and phenanthrene

449   methanols. Antimicrob Agents Chemother **1998**; 42:2973-7.

450   8.   Fitch, C.D. Ferriprotoporphyrin IX, phospholipids, and the antimalarial actions of

451   quinoline drugs. Life Sci **2004**; 74:1957-72.

452   9.   Naude, B., J.A. Brzostowski, A.R. Kimmel, T.E. Wellems. *Dictyostelium discoideum*

453   expresses a malaria chloroquine resistance mechanism upon transfection with mutant,

454   but not wild-type, *Plasmodium falciparum* transporter PfCRT. J Biol Chem **2005**;

455   280:25596-25603.

456   10.   Sanchez, C.P., J.E. McLean, P. Rohrbach, D.A. Fidock, W.D. Stein, M. Lanzer. Evidence for

457   a *pfcrt*-associated chloroquine efflux system in the human malarial parasite

458   *Plasmodium falciparum*. Biochemistry **2005**; 44:9862-70.

459   11.   Lehane, A.M., K. Kirk. Chloroquine resistance-conferring mutations in *pfcrt* give rise to

460   a chloroquine-associated H^+ leak from the malaria parasite's digestive vacuole.

461   Antimicrob Agents Chemother **2008**; 52:4374-80.

462   12.   Lehane, A.M., K. Kirk. Efflux of a range of antimalarial drugs and 'chloroquine

463   resistance reversers' from the digestive vacuole in malaria parasites with mutant

464   PfCRT. Mol Microbiol **2010; 77:1039-51**.

465   13.   Martin, R.E., R.V. Marchetti, A.I. Cowan, S.M. Howitt, S. Bröer, K. Kirk. Chloroquine

466   transport via the malaria parasite's chloroquine resistance transporter. Science **2009**;

467   325:1680-2.

468   14.   Bellanca, S., R.L. Summers, M. Meyrath, et al. Multiple drugs compete for transport via

469   the *Plasmodium falciparum* chloroquine resistance transporter at distinct but

470   interdependent sites. J Biol Chem **2014**; 289:36336-51.

471   15.   Summers, R.L., A. Dave, T.J. Dolstra, et al. Diverse mutational pathways converge on

472   saturable chloroquine transport via the malaria parasite's chloroquine resistance

473   transporter. Proc Natl Acad Sci U S A **2014**; 111:E1759-67.

474   16.   Buchholz, K., R.H. Schirmer, J.K. Eubel, et al. Interactions of methylene blue with human

475   disulfide reductases and their orthologues from *Plasmodium falciparum*. Antimicrob

476   Agents Chemother **2008**; 52:183-91.

477   17.   Atamna, H., M. Krugliak, G. Shalmiev, E. Deharo, G. Pescarmona, H. Ginsburg. Mode of

478   antimalarial effect of methylene blue and some of its analogues on *Plasmodium*

479   *falciparum* in culture and their inhibition of *P. vinckei petteri* and *P. yoelii nigeriensis in*

480   *vivo*. Biochem Pharmacol **1996**; 51:693-700.

481 18. Blank, O., E. Davioud-Charvet, M. Elhabiri. Interactions of the antimalarial drug

482   methylene blue with methemoglobin and heme targets in *Plasmodium falciparum*: a

483   physico-biochemical study. Antioxid Redox Signal **2012**; 17:544-54.

484 19. Ginsburg, H., E. Nissani, M. Krugliak. Alkalinization of the food vacuole of malaria

485   parasites by quinoline drugs and alkylamines is not correlated with their antimalarial

486   activity. Biochem Pharmacol **1989**; 38:2645-54.

487 20. Keiser, J., J. Utzinger, Z. Premji, Y. Yamagata, B.H. Singer. Acridine Orange for malaria

488   diagnosis: its diagnostic performance, its promotion and implementation in Tanzania,

489   and the implications for malaria control. Ann Trop Med Parasitol **2002**; 96:643-54.

490 21. Bennett, T.N., A.D. Kosar, L.M. Ursos, et al. Drug resistance-associated pfCRT mutations

491   confer decreased *Plasmodium falciparum* digestive vacuolar pH. Mol Biochem Parasitol

492   **2004**; 133:99-114.

493 22. Ursos, L.M., S.M. Dzekunov, P.D. Roepe. The effects of chloroquine and verapamil on

494   digestive vacuolar pH of *P. falciparum* either sensitive or resistant to chloroquine. Mol

495   Biochem Parasitol **2000**; 110:125-34.

496 23. Dzekunov, S.M., L.M. Ursos, P.D. Roepe. Digestive vacuolar pH of intact

497   intraerythrocytic *P. falciparum* either sensitive or resistant to chloroquine. Mol

498   Biochem Parasitol **2000**; 110:107-24.

499 24. Hayward, R., K.J. Saliba, K. Kirk. The pH of the digestive vacuole of *Plasmodium*

500   *falciparum* is not associated with chloroquine resistance. J Cell Sci **2006**; 119:1016-25.

501 25. Kumar, S., M. Guha, V. Choubey, P. Maity, U. Bandyopadhyay. Antimalarial drugs

502   inhibiting hemozoin (beta-hematin) formation: a mechanistic update. Life Sci **2007**;

503   80:813-28.

504 26. Ehrhardt, K., E. Davioud-Charvet, H. Ke, A.B. Vaidya, M. Lanzer, M. Deponte. The

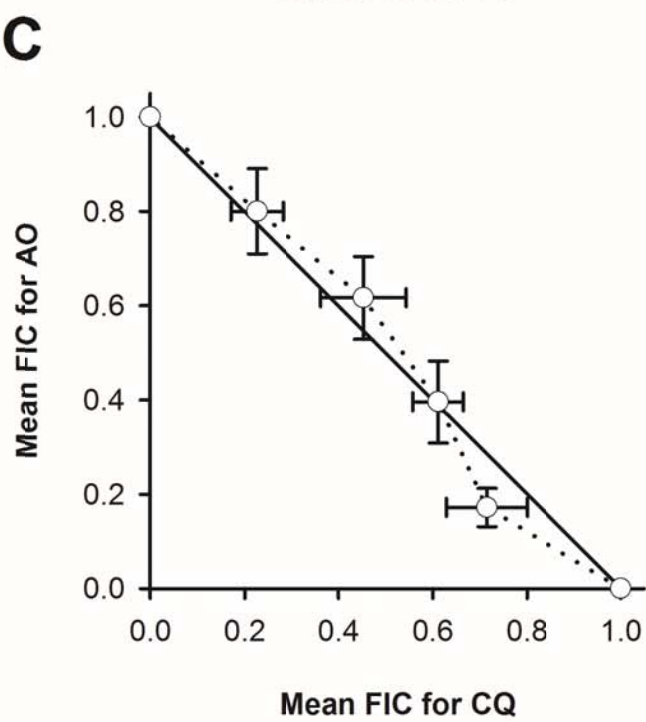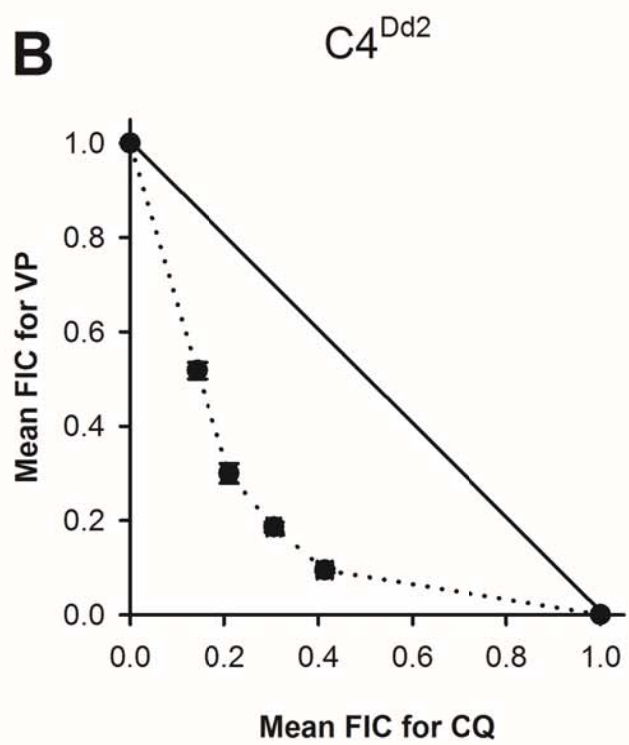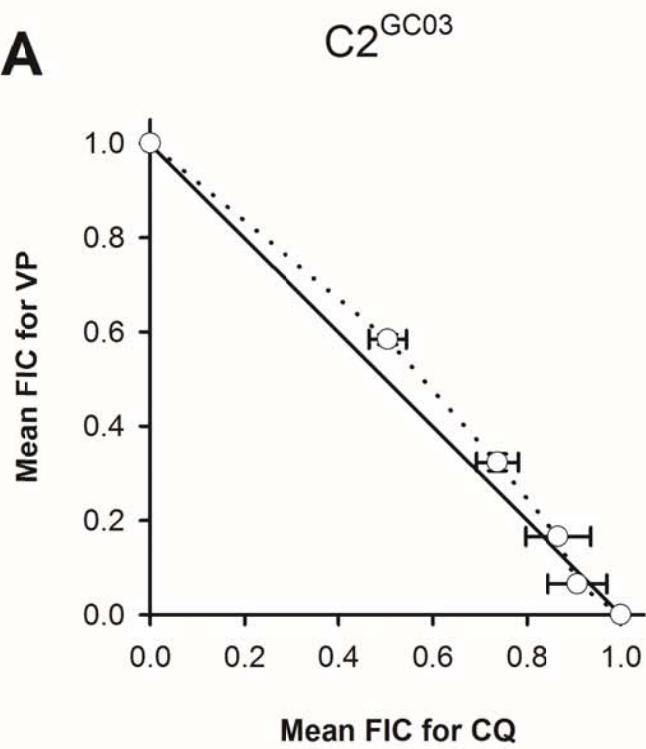505   antimalarial activities of methylene blue and the 1,4-naphthoquinone 3-[4-

506   (trifluoromethyl)benzyl]-menadione are not due to inhibition of the mitochondrial

507   electron transport chain. Antimicrob Agents Chemother **2013**; 57:2114-20.

508 27. Kelly, J.X., M.J. Smilkstein, R. Brun, et al. Discovery of dual function acridones as a new

509   antimalarial chemotype. Nature **2009**; 459:270-3.

510 28. Valdes, A.F. Acridine and acridinones: old and new structures with antimalarial

511   activity. Open Med Chem J **2011**; 5:11-20.

512 29. Adjalley, S.H., G.L. Johnston, T. Li, et al. Quantitative assessment of *Plasmodium*

513   *falciparum* sexual development reveals potent transmission-blocking activity by

514   methylene blue. Proc Natl Acad Sci U S A **2011**; 108:E1214-23.

515 30. Coulibaly, B., A. Zoungrana, F.P. Mockenhaupt, et al. Strong gametocytocidal effect of

516   methylene blue-based combination therapy against *falciparum* malaria: a randomised

517   controlled trial. PLoS One **2009**; 4:e5318.

518 31. Zoungrana, A., B. Coulibaly, A. Sie, et al. Safety and efficacy of methylene blue combined

519   with artesunate or amodiaquine for uncomplicated *falciparum* malaria: a randomized

520   controlled trial from Burkina Faso. PLoS One **2008**; 3:e1630.

521 32. Coulibaly, B., M. Pritsch, M. Bountogo, et al. Efficacy and safety of triple combination

522   therapy with artesunate-amodiaquine-methylene blue for *falciparum* malaria in

523   children: a randomized controlled trial in Burkina Faso. J Infect Dis **2015**; 211:689-97.

524 33. Muller, O., F.P. Mockenhaupt, B. Marks, et al. Haemolysis risk in methylene blue

525   treatment of G6PD-sufficient and G6PD-deficient West-African children with

526   uncomplicated *falciparum* malaria: a synopsis of four RCTs. Pharmacoepidemiol Drug

527   Saf **2013**; 22:376-85.

528 34. Anderson, M.O., J. Sherrill, P.B. Madrid, et al. Parallel synthesis of 9-aminoacridines and

529   their evaluation against chloroquine-resistant *Plasmodium falciparum*. Bioorg Med
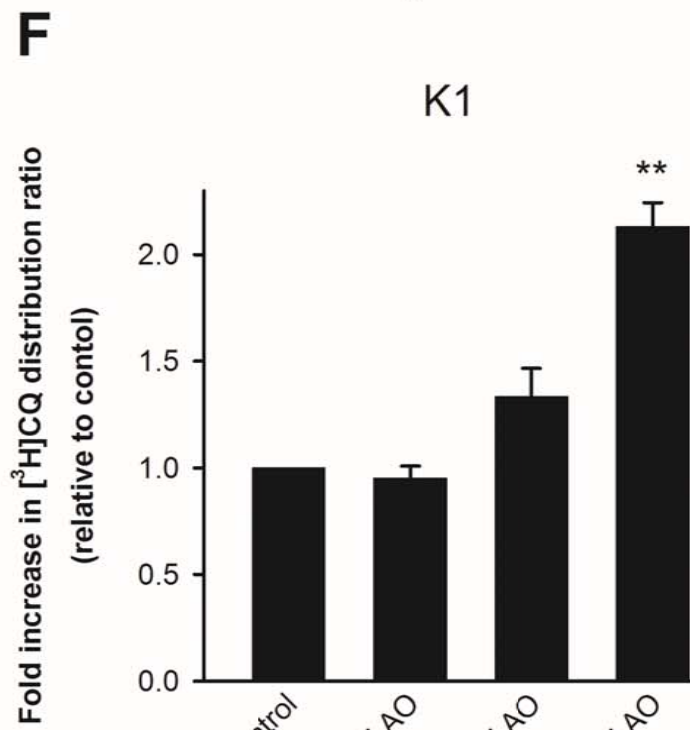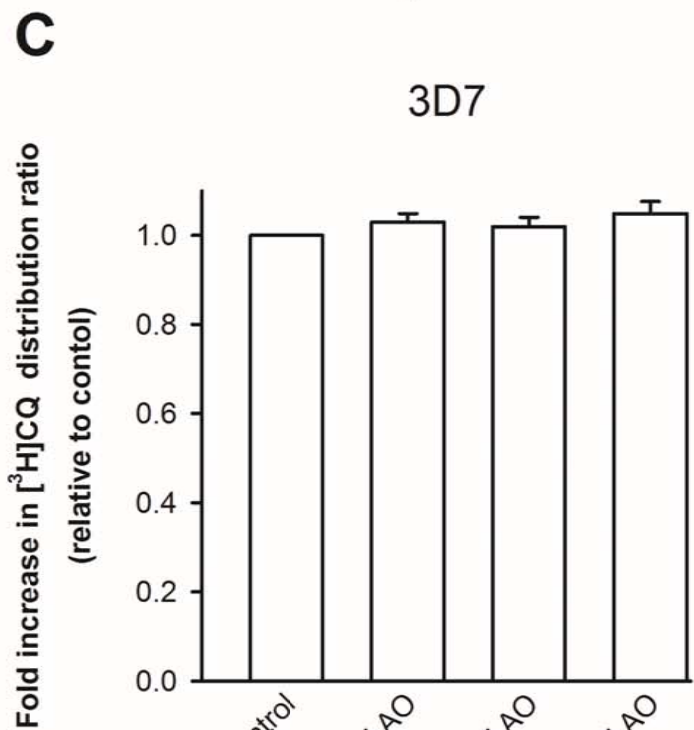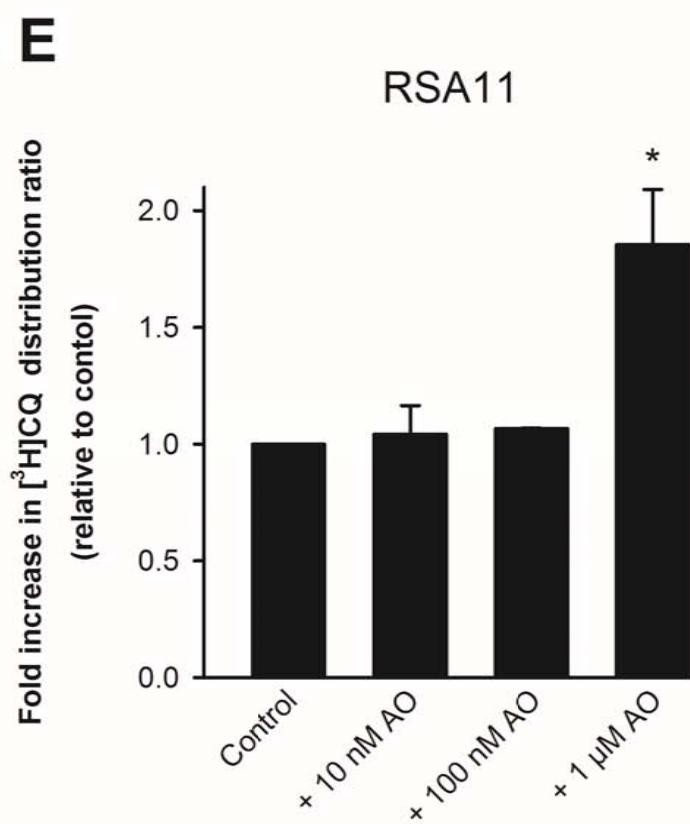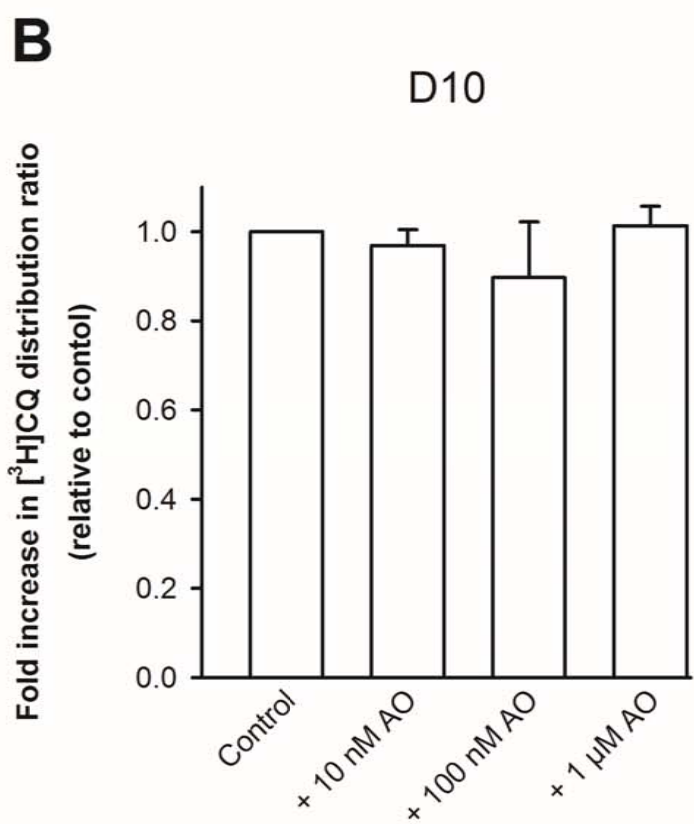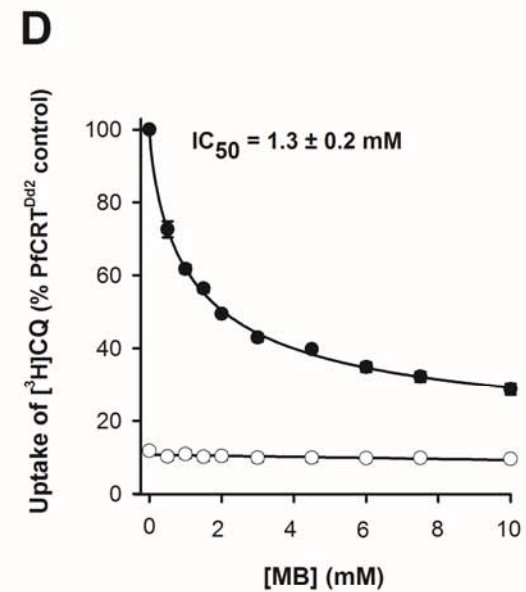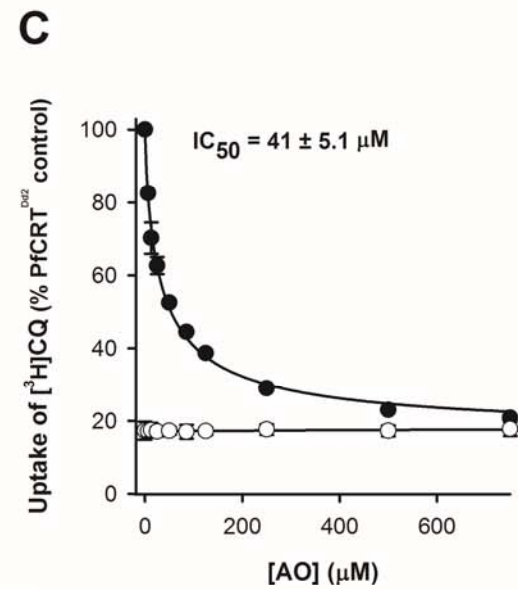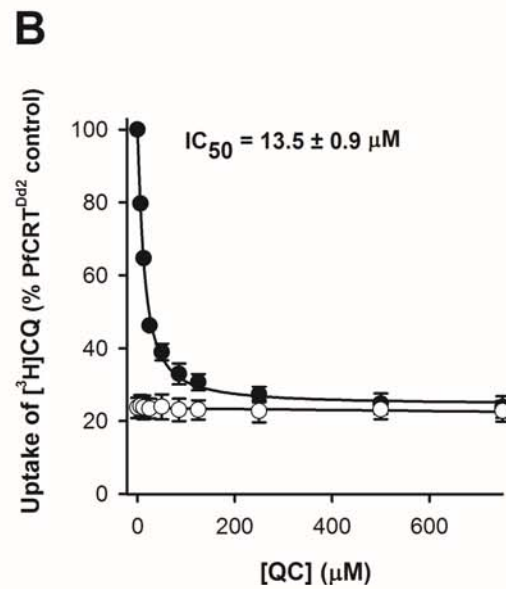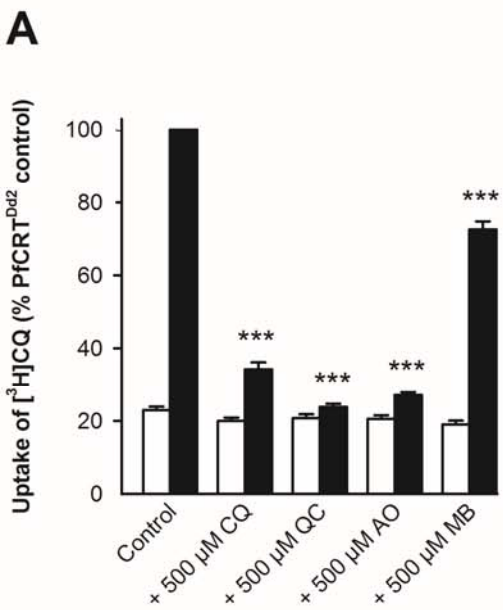
530   Chem **2006**; 14:334-43.

531   35.   Elueze, E.I., S.L. Croft, D.C. Warhurst. Activity of pyronaridine and mepacrine against

532   twelve strains of *Plasmodium falciparum in vitro*. J Antimicrob Chemother **1996**;

533   37:511-8.

534   36.   Hawley, S.R., P.G. Bray, M. Mungthin, J.D. Atkinson, P.M. O'Neill, S.A. Ward. Relationship

535   between antimalarial drug activity, accumulation, and inhibition of heme

536   polymerization in *Plasmodium falciparum in vitro*. Antimicrob Agents Chemother

537   **1998**; 42:682-6.

538   37.   Sanchez, C.P., J.E. McLean, W. Stein, M. Lanzer. Evidence for a substrate specific and

539   inhibitable drug efflux system in chloroquine resistant *Plasmodium falciparum* strains.

540   Biochemistry **2004**; 43:16365-73.

541   38.   Pascual, A., M. Henry, S. Briolant, et al. *In vitro* activity of Proveblue (methylene blue)

542   on *Plasmodium falciparum* strains resistant to standard antimalarial drugs. Antimicrob

543   Agents Chemother **2011**; 55:2472-4.

544   39.   Vennerstrom, J.L., M.T. Makler, C.K. Angerhofer, J.A. Williams. Antimalarial dyes

545   revisited: xanthenes, azines, oxazines, and thiazines. Antimicrob Agents Chemother

546   **1995**; 39:2671-7.

547   40.   Okombo, J., S.M. Kiara, L. Mwai, et al. Baseline *in vitro* activities of the antimalarials

548   pyronaridine and methylene blue against *Plasmodium falciparum* isolates from Kenya.

549   Antimicrob Agents Chemother **2012**; 56:1105-7.

550   41.   Wirjanata, G., B.F. Sebayang, F. Chalfein, et al. Potent *ex vivo* activity of naphthoquine

551   and methylene blue against drug resistant clinical isolates of *Plasmodium falciparum*

552   and *Plasmodium vivax*. Antimicrob Agents Chemother **2015**; 59:6117-24.

553   42.   Akoachere, M., K. Buchholz, E. Fischer, et al. *In vitro* assessment of methylene blue on

554   chloroquine-sensitive and -resistant *Plasmodium falciparum* strains reveals synergistic

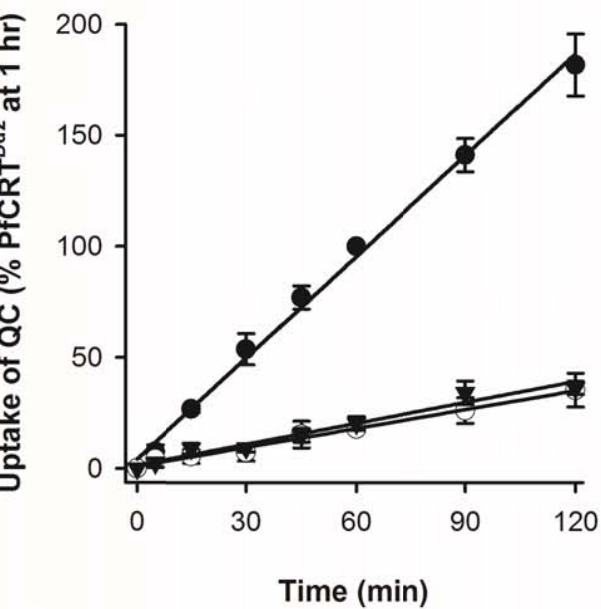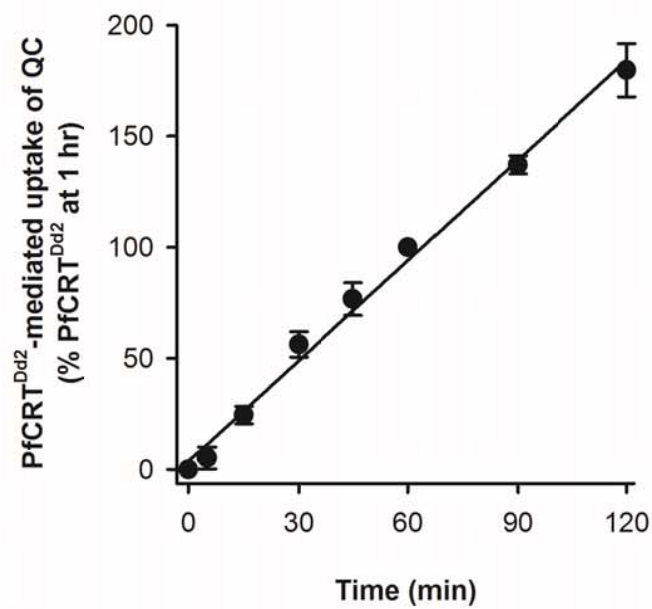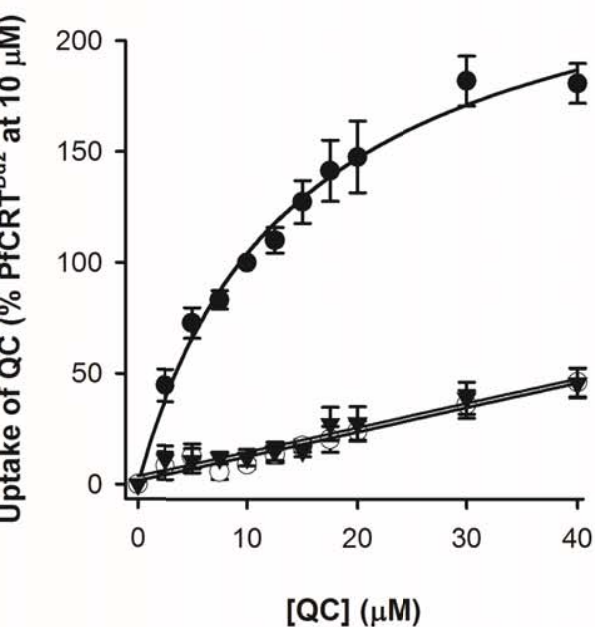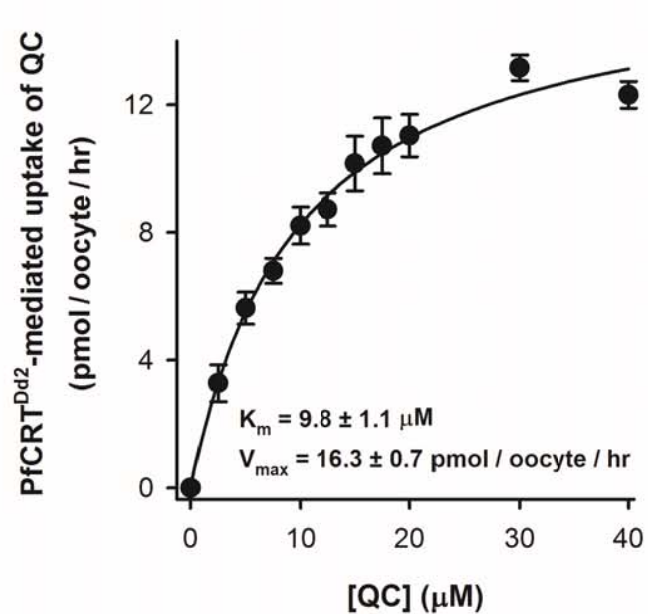555   action with artemisinins. Antimicrob Agents Chemother **2005**; 49:4592-7.
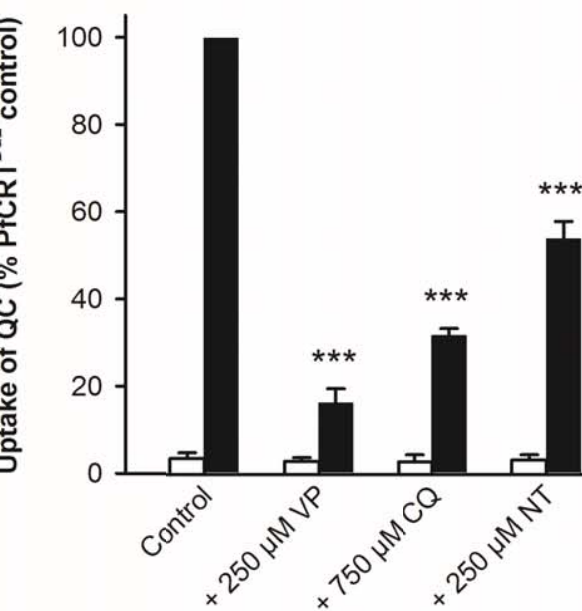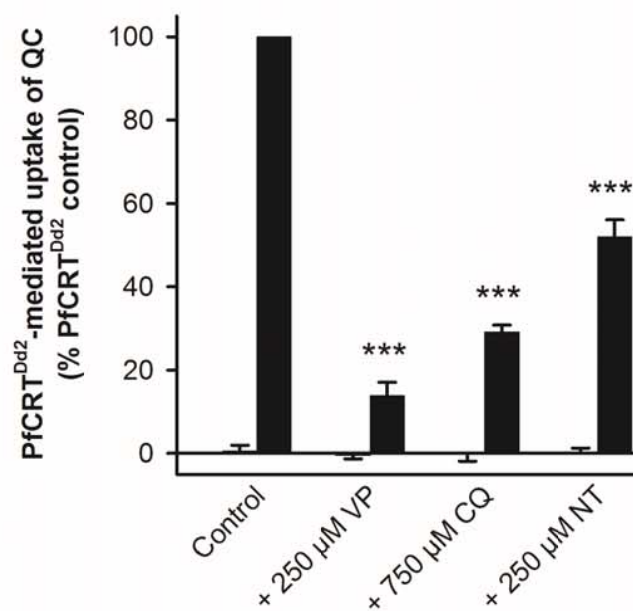
556   43.   Sidhu, A.B., D. Verdier-Pinard, D.A. Fidock. Chloroquine resistance in *Plasmodium*

557   *falciparum* malaria parasites conferred by *pfcrt* mutations. Science **2002**; 298:210-3.

558   44.   Martin, S.K., A.M. Oduola, W.K. Milhous. Reversal of chloroquine resistance in

559   *Plasmodium falciparum* by verapamil. Science **1987**; 235:899-901.

560   45.   Deane, K.J., R.L. Summers, A.M. Lehane, R.E. Martin, R.A. Barrow. Chlorpheniramine

561   Analogues Reverse Chloroquine Resistance in *Plasmodium falciparum* by Inhibiting

562   PfCRT. ACS Med Chem Lett **2014**; 5:576-81.

563   46.   Martin, R.E., A.S. Butterworth, D.L. Gardiner, K. Kirk, J.S. McCarthy, T.S. Skinner-Adams.

564   Saquinavir inhibits the malaria parasite's chloroquine resistance transporter.

565   Antimicrob Agents Chemother **2012**; 56:2283-9.

566   47.   Sa, J.M., O. Twu, K. Hayton, et al. Geographic patterns of *Plasmodium falciparum* drug

567   resistance distinguished by differential responses to amodiaquine and chloroquine.

568   Proc Natl Acad Sci U S A **2009**; 106:18883-9.

569   48.   Hanssen, E., C. Knoechel, M. Dearnley, et al. Soft X-ray microscopy analysis of cell

570   volume and hemoglobin content in erythrocytes infected with asexual and sexual

571   stages of *Plasmodium falciparum*. J Struct Biol **2012**; 177:224-32.

572   49.   Silvestrini, F., E. Lasonder, A. Olivieri, et al. Protein export marks the early phase of

573   gametocytogenesis of the human malaria parasite *Plasmodium falciparum*. Mol Cell

574   Proteomics **2010**; 9:1437-48.

575   50.   Summers, R.L., R.E. Martin. Functional characteristics of the malaria parasite's

576   "chloroquine resistance transporter": implications for chemotherapy. Virulence **2010**;
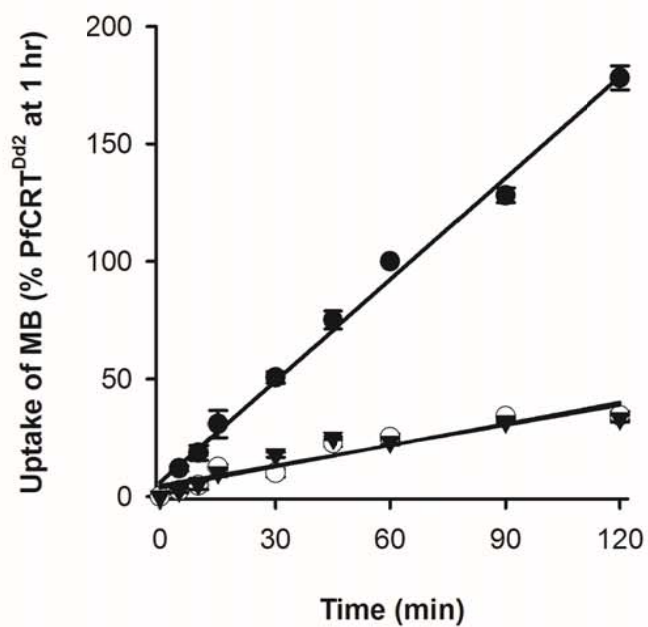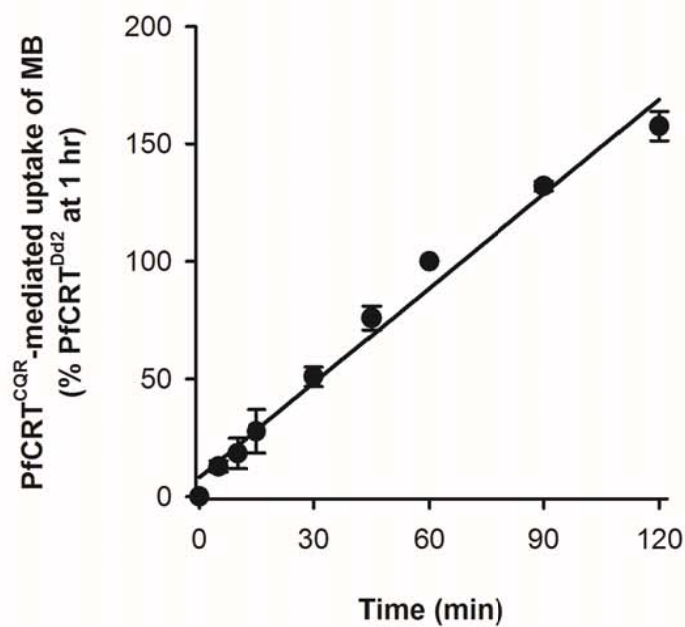
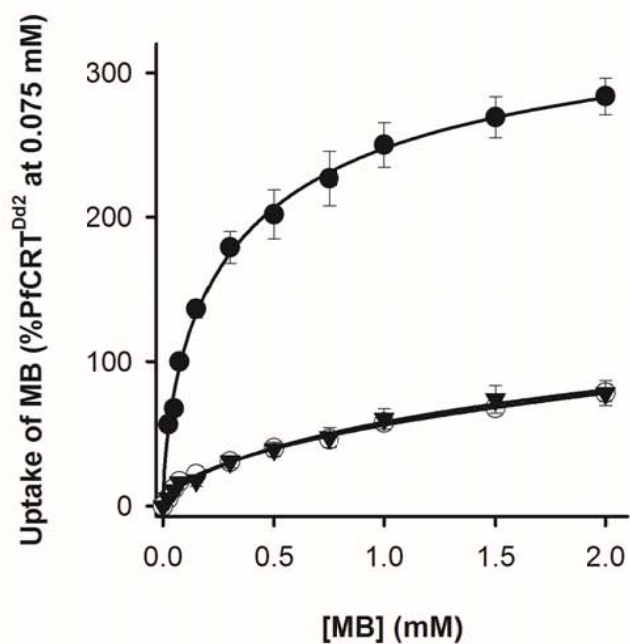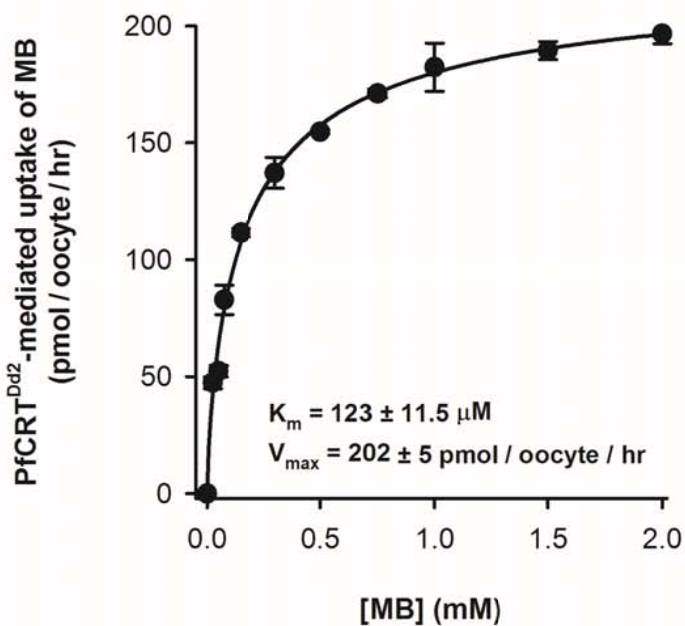577   1:304-8.

578

B D10

C 3D7

E RSA11

F K1

A

Uptake of [^{3}H]CQ (% PfCRT^{Dd2} control)

Control
+ 500 μM CQ ***
+ 500 μM QC ***
+ 500 μM AO ***
+ 500 μM MB ***

B

Uptake of [^{3}H]CQ (% PfCRT^{Dd2} control)

[QC] (μM)

IC$_{50}$ = 13.5 ± 0.9 μM

C

Uptake of [^{3}H]CQ (% PfCRT^{Dd2} control)

[AO] (μM)

IC$_{50}$ = 41 ± 5.1 μM

D

Uptake of [^{3}H]CQ (% PfCRT^{Dd2} control)

[MB] (mM)

IC$_{50}$ = 1.3 ± 0.2 mM
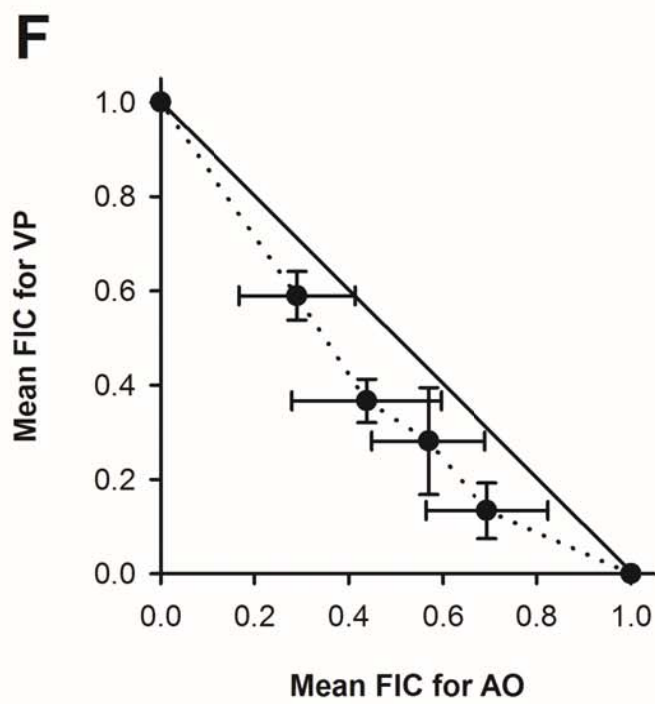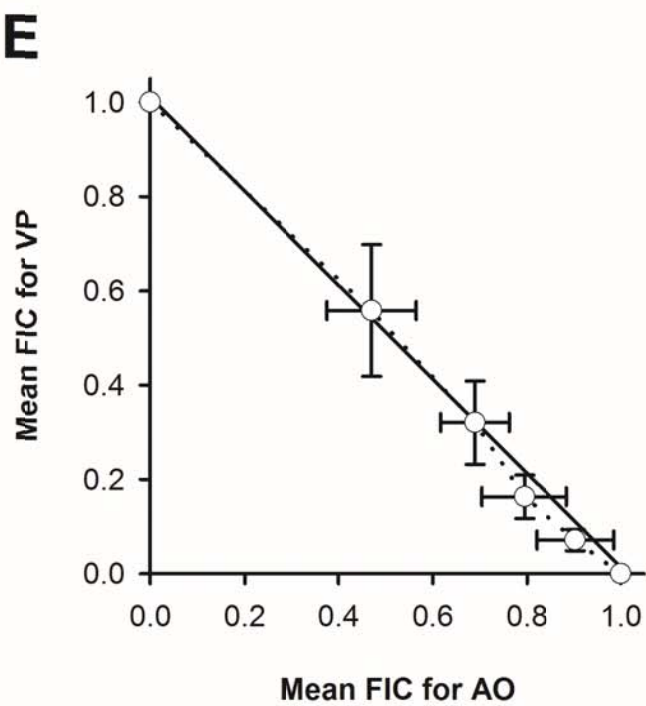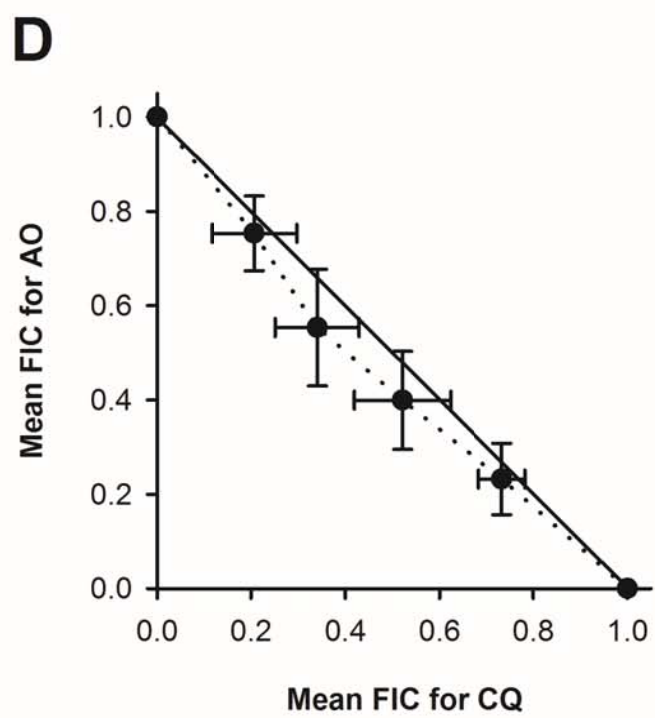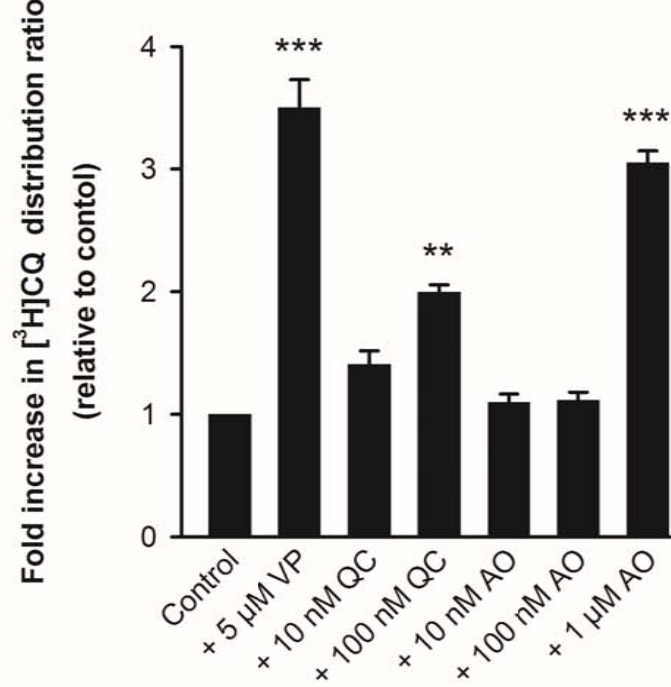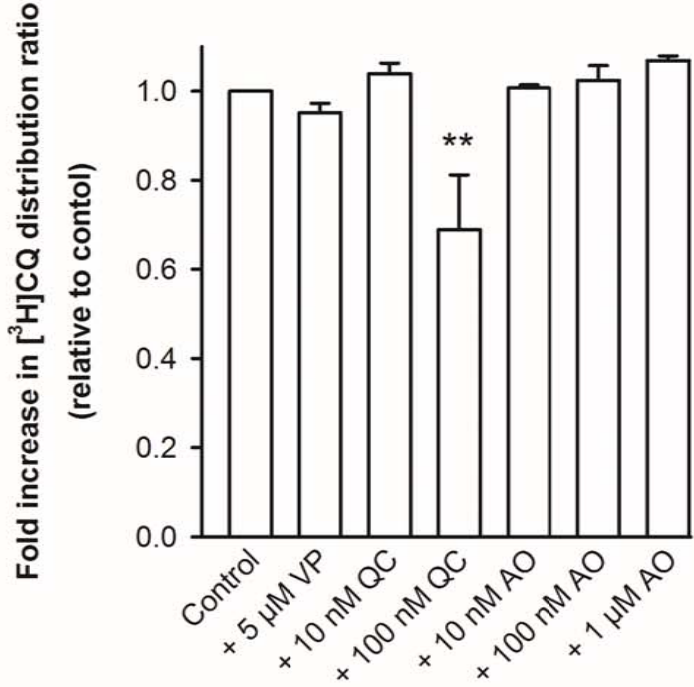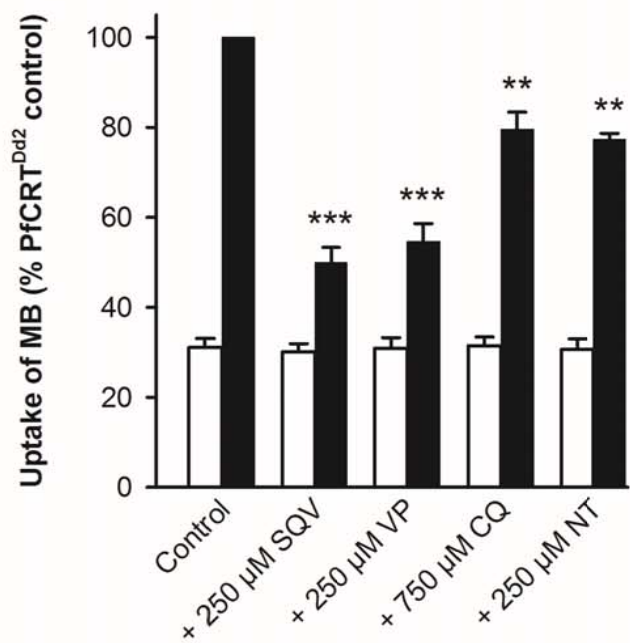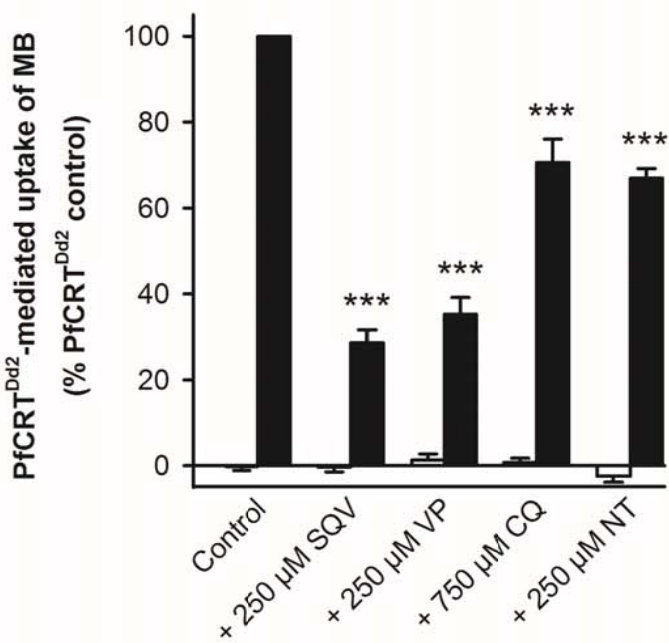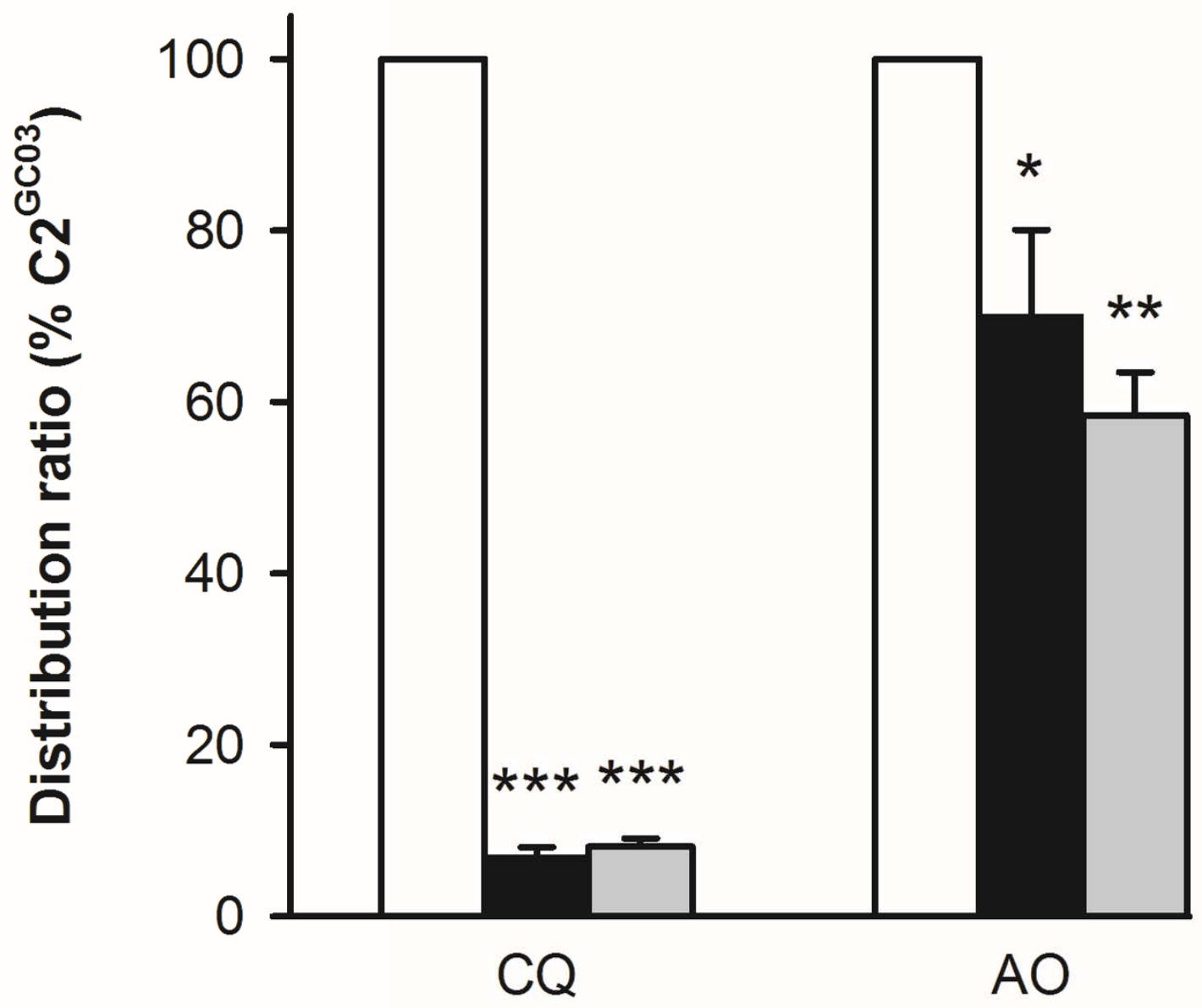
Table

Table 1. In Vitro Antiplasmodial Activities of Chloroquine (CQ), Quinacrine (QC), Acridine Orange (AO), and Methylene Blue (MB) against CQ-Sensitive and CQ-Resistant *P. falciparum* Parasites

| Strain/ line[b] | IC_{50} (nM)[a] | | | | | | | |
| | Chloroquine | | Quinacrine | | Acridine orange | | Methylene blue | |
	Control	+ 1 µM VP	Control	+ 1 µM VP	Control	+ 1 µM VP	Control	+ 1 µM VP
D10	26 ± 2.6	27 ± 2.5	-	-	288 ± 20	283 ± 63	-	-
3D7	21 ± 0.5	20 ± 0.6	9.8 ± 0.2	9.9 ± 0.2	309 ± 34	294 ± 24	2.6 ± 0.04	2.5 ± 0.08
RSA11	354 ± 39[c]	43 ± 5.5[f]	-	-	586 ± 39[e]	563 ± 84	-	-
K1	255 ± 26[c]	63 ± 8.4[f]	-	-	652 ± 42[c]	644 ± 98	-	-
Dd2	142 ± 7.2[c]	26 ± 2.4[f]	16 ± 1.4[d]	7.9 ± 0.6[f]	606 ± 19[d]	549 ± 30	5.3 ± 0.06[c]	2.3 ± 0.08[f]
C2^{GC03}	8.3 ± 0.4	8.4 ± 0.2	9.9 ± 0.8	10 ± 0.2	373 ± 28	268 ± 42	2.5 ± 0.03	2.1 ± 0.1
C4^{Dd2}	130 ± 9.7[c]	47 ± 8.1[f]	19 ± 0.6[c]	8.9 ± 1.1[f]	592 ± 56[d]	610 ± 27	4.3 ± 0.4[c]	1.9 ± 0.02[f]
C6^{7G8}	89 ± 4.1[c]	24 ± 2.9[g]	14 ± 0.8[d]	11 ± 0.2[h]	491 ± 19	501 ± 20	4.7 ± 0.05[c]	2.5 ± 0.03[f]

Abbreviations: IC_{50}, half-maximal inhibitory concentrations; VP, verapamil.

[a]The IC_{50}s are shown as the mean ± SEM from 3 to 11 independent experiments (performed on different days), within which measurements were averaged from 2 or 3 replicates.

[b]Field-derived CQ-sensitive strains: D10 (Papua New Guinea); 3D7 (Africa). Field-derived CQ-resistant strains: RSA11 (South Africa); K1 (Thailand); Dd2 (Indochina/Laos). Isogenic *pfcrt* transfectant lines: C2^{GCO3} (CQ-sensitive); C4^{Dd2} (CQ-resistant); C6^{7G8} (CQ-resistant).

P values determined from Student *t*-test comparisons with the relevant CQ-sensitive strain or line (and within the same drug treatment) were less than [c]0.001, [d]0.01, or [e]0.05.

P values determined from Student *t*-test comparisons with the control treatment from the same CQ-sensitive strain or line (and within the same drug treatment) were less than [f]0.001, [g]0.01, or [h]0.05.

Supplementary Materials for

Verapamil-sensitive transport of quinacrine and methylene blue via mutant

PfCRT reduces the malaria parasite's susceptibility to these tricyclic drugs

Donelly A. van Schalkwyk[a], Megan N. Nash[a], Sarah H. Shafik[a], Robert L. Summers, Adele M.

Lehane, Peter J. Smith, and Rowena E. Martin*

[a]D. A. vS., M. N. N., and S. H. S. contributed equally to this work.

*Correspondence: Rowena Martin, Research School of Biology, Australian National University,

Canberra, ACT, 2601, Australia (rowena.martin@anu.edu.au).

This PDF file includes:

Supplementary Materials and Methods

Supplementary Tables 1 and 2

Supplementary Figures 1, 2, and 3

References

Supplementary Materials and Methods

Measurements of *P. falciparum* Drug Susceptibility

Parasite proliferation was measured in 96-well plates using either the [3H]hypoxanthine incorporation method or the lactate dehydrogenase (pLDH) assay. The [3H]hypoxanthine incorporation assay was performed over 72 hours using a protocol described elsewhere [1], and the starting hematocrit and parasitemia were both approximately 1%. The Malstat™ reagent (Flow Inc.) was used to measure pLDH activity in accordance with the method of Makler and colleagues [2], and these assays were performed over 48 hours with a starting hematocrit and parasitemia of approximately 1% and 2%, respectively. The level of parasite proliferation in the presence of each drug concentration was expressed as a percentage of the proliferation measured in the absence of drug. The IC_{50} (i.e., the concentration of drug at which the inhibition of parasite growth is half-maximal) was determined in SigmaPlot by a least-squares fit of the equation $y = a/[1+([drug]/IC_{50})c]$ to the data, where y is the percent parasite proliferation, a is the maximum change in the percent parasite proliferation, and c is a fitted constant. The IC_{50}s obtained using the [3H]hypoxanthine incorporation method were indistinguishable from those generated with the pLDH assay.

Antimalarial drug combinations were assessed using fixed-ratio isobolograms [3] as described previously [4]. Fractional inhibitory concentrations (FICs) were calculated for each drug within a combination as follows: FIC (A) = the IC_{50} for drug A in a combination divided by the IC_{50} for drug A alone; FIC (B) = the IC_{50} for drug B in a combination divided by the IC_{50} for drug B alone. The isobolograms were constructed by plotting FIC (A) against FIC (B) for each combination. It is generally accepted that a drug combination is synergistic if the FIC is ≤ 0.5, antagonistic if the FIC is ≥ 4.0 [5], and additive if the FIC is not significantly different from 1.

In all cases, at least three independent experiments were performed (on different days), and within each experiment measurements were averaged from three replicates.

P. falciparum **Drug Accumulation Assays**

The accumulation of [^{3}H]CQ and [^{3}H]AO was measured in mature trophozoite-infected erythrocytes (~36 hours post-invasion). In the experiments giving rise to the data presented in Figure 2, hematocrit and parasitaemia were approximately 1% and 5%, respectively, and the initial extracellular concentration of [^{3}H]CQ was 2 nM (7 Ci/mmol; Moravek Biochemicals). Prior to the addition of [^{3}H]CQ, the cell suspension was incubated for 15 minutes at 37°C in the presence or absence of the test compound (unlabelled VP, AO, or QC). The 1-hour incubation was terminated by the addition of 100 μL of dibutyl phthalate to the cell suspension and immediate centrifugation ($17000 \times g$, 1 minute) to sediment the cells. The supernatant solution was aspirated and the microcentrifuge tube tip containing the pelleted cells was cut off and placed in a scintillation vial (PerkinElmer). The cells were lysed with 100 μL of Solvable (Packard; 30 minutes at room temperature) and the sample decolourised by the addition of 100 μL of hydrogen peroxide (Sigma; 30 minutes at room temperature). Scintillation fluid (2 mL of Ultima Gold; PerkinElmer) was added to each vial and the samples were shaken overnight. The radioactivity was measured with a Packard Tri-Carb 4640 liquid scintillation analyser. The data presented in panels *A* and *D* of Figure 2 were derived from three independent experiments (performed on different days), within which measurements were averaged from three replicates. Panels *B*, *C*, *E*, and *F* of Figure 2 show the mean of two independent experiments (performed on different days), within which measurements were averaged from three replicates.

The experiments giving rise to the data presented in Figure 6 and Supplementary Figure 3 were performed according to a protocol described in detail elsewhere [6] with minor modifications. Briefly, the hematocrit was 2% and the parasitaemia ranged between 3.2 and

8.4%, and the initial extracellular concentrations of [3H]CQ (20 Ci/mmol) and [3H]AO (25 Ci/mmol) (both from American Radiolabeled Chemicals, ARC) were 20 nM and 50 nM, respectively. The 1-hour incubation at 37°C was terminated by transferring an aliquot of the suspension (200 μL, in duplicate) to a microcentrifuge tube containing 300 μL of dibutyl phthalate (Sigma-Aldrich), which was centrifuged immediately ($17,000 \times g$, 2 minutes) to sediment the cells. The supernatant solution was removed by aspiration and residual radioactivity on the sides of the tube was removed by rinsing four times with water, after which the majority of the dibutyl phthalate was aspirated. The cell pellet was dissolved in 1 M NaOH (100 μL, 2 hours at 55°C) and the sample decolourised by the addition of 12.5% w/v bleach (25 μL, 2 hours at room temperature) prior to dilution with water (1 mL). The sample was then transferred to a scintillation vial, mixed with scintillation fluid (1.5 mL of Irga-Safe Plus; PerkinElmer), and the radioactivity measured with a PerkinElmer Tri-Carb 2810 liquid scintillation analyser. The data presented in Figure 6 were derived from four independent experiments (performed on different days), within which measurements were averaged from two replicates.

In all cases, the drug accumulation ratio (i.e., the concentration of [3H]drug within the infected cells relative to the concentration in the extracellular medium) was calculated using a previous estimate of the water volume of a trophozoite-infected erythrocyte (75 fL) [7].

Harvest, Preparation and Microinjection of *X. laevis* Oocytes

Ethical approval of the work performed with the *X. laevis* frogs was obtained from the Australian National University Animal Experimentation Ethics Committee (Animal Ethics Protocol Number A2013/13) in accordance with the Australian Code of Practice for the Care and Use of Animals for Scientific Purposes. Sections of ovary were surgically removed using a procedure adapted from the Laboratory *Xenopus* handbook [8]. Adult female *X. laevis* frogs (purchased from NASCO) were anaesthetised by submersion in a solution of ethyl 3-

aminobenzoate methanesulfonate salt (1.6 g/L of tap water; Sigma-Aldrich) and 1 mM NaHCO$_3$ (Sigma-Aldrich). Anaesthesia was complete after approximately 20 minutes, or when the frog could be turned onto its back without eliciting a response. The frog was then placed onto a container of ice covered with two sheets of moist paper towel. A moist sheet of paper towel was also placed over the frog's head and another over its legs, leaving the abdomen exposed. Ice was piled onto the frog's head and legs to prevent bleeding. After the abdomen was swabbed with a cotton bud sprayed with 80% ethanol, a sterile scalpel was used to make a 1 cm incision directly above the position of an ovary – first through the skin and then though the muscle layer. Sections of the ovary were removed with sterile, surgical-grade tweezers and scissors and placed in a pre-weighed petri dish containing 'calcium-free oocyte ringer' (OR^{2-}) buffer (82.5 mM NaCl, 2.5 mM KCl, 1 mM MgCl$_2$, 1 mM Na$_2$HPO$_4$, 5 mM HEPES; pH 7.8). The incision was closed with one stitch of absorbable suture (B. Braun) in the muscle layer, and two stiches of non-absorbable suture (B. Braun) in the skin layer. The wound was swabbed with a cotton bud sprayed with 80% ethanol, after which the frog was returned to an empty tank. The frog then recovered under a sheet of moist paper towel, and was submersed in tap water once fully awake.

The petri dish was re-weighed and the mass of the ovary calculated. The ovary sections were cut into pieces containing around 200 oocytes. If the total mass of the ovary tissue was 17 g or less, the sections were transferred to a 100 mL Erlenmeyer flask, whereas a 250 mL Erlenmeyer flask was used when the total mass was greater than 17 g. The ovary pieces were washed with OR^{2-} buffer (five times, or until the buffer was no longer cloudy) before being incubated for 16 hours at 16°C on an orbital shaker in OR^{2-} buffer supplemented with 0.5 M Na$_2$HPO$_4$ (Sigma-Aldrich), bovine serum albumin (250 mg/mL, Sigma-Aldrich), and collagenase D (Roche). The volume of the buffer was 25 mL and 50 mL for the 100 mL and 250 mL flasks, respectively. The amount of collagenase D added to the solution was described by the equation $y = 0.44x + 11.5$, where x was the mass of ovary tissue in g and y was the mass

of collagenase in mg. This ratio of collagenase D to ovary mass typically produced good yields of healthy, single, and de-folliculated oocytes when the ovary mass ranged from 11 to 24 g. The collagenase-treated oocytes were washed ten times with OR^{2-} buffer and five times with 'calcium-containing oocyte ringer' (OR^{2+}) buffer (OR^{2-} buffer supplemented with 1 mM $CaCl_2$ and 50 µg/mL gentamycin). An ovary mass of 14-20 g usually yielded 2000-5000 healthy, de-folliculated oocytes of a suitable size and age (developmental stages V and VI) for microinjection with cRNA (20 ng per oocyte) encoding PfCRT. The injections were performed using a Nanoliter 2000 Injector and Micro4 Controller (World Precision Instruments) with fine-tipped glass capillaries that were shaped on a Flaming/Brown micropipette puller (Sutter Instrument Co.). Oocytes were stored at 16-18°C in OR^{2+} buffer (which was replaced daily) and the solute uptake experiments were performed 3-6 days post-injection.

Measurements of Drug Transport in *Xenopus* Oocytes

The direction of drug transport in the PfCRT oocyte expression system is from the acidic extracellular medium (pH 5.0 to 6.0) into the oocyte cytosol (pH 7.2) [9], which corresponds to the efflux of drug from the acidic digestive vacuole (pH 5 to 5.5) [10-12] into the parasite cytosol (pH 7.3) [13]. A key advantage of this system is that it allows PfCRT to be studied directly and in isolation, without confounding effects such as the binding of drugs to heme or interactions of the compound with other targets or transporters.

Unless specified otherwise, the drug influx assays were performed over 1-2 hours at 27.5°C and in ND96 buffer (96 mM NaCl, 2 mM KCl, 1 mM $MgCl_2$, 1.8 mM $CaCl_2$, 10 mM MES, and 10 mM Tris-base). The uptake of [³H]CQ (0.25 µM; 20 Ci/mmol; ARC) was measured at pH 6.0 and in the presence of 15 µM unlabelled CQ. A subset of experiments attempted to measure the transport of [³H]AO (0.2 µM; 25 Ci/mmol; ARC) into oocytes in the presence of unlabelled AO (1, 2.5, 5, or 10 µM) at pH 4.5, 5.0, 5.5, and 6.0. For each treatment, 10 oocytes were transferred to a 5 mL polystyrene round bottom tube (Falcon) and washed twice with

3.5 mL of ND96 buffer, with the residual buffer removed by pipette. Influx commenced with the addition of 100 μL of ND96 buffer supplemented with [³H]CQ (or [³H]AO), unlabelled CQ (or AO) and, where specified, an unlabelled inhibitor (e.g., QC, AO, MB, or VP). The assay was terminated by removing the reaction buffer with a pipette and washing the oocytes twice with 3.5 mL of ice-cold ND96 buffer. Each oocyte was transferred to a separate scintillation vial and incubated overnight at room temperature in 200 μL of 10% SDS (Sigma-Aldrich). The lysed oocyte was then combined with 1.5 mL of Irga-Safe Plus and the radioactivity measured with a PerkinElmer Tri-Carb 2810 liquid scintillation analyser.

The IC$_{50}$ values presented in Figures 3B-D were determined in SigmaPlot by a least-squares fit of the equation $y = y_{min} + [(y_{max} - y_{min})/(1 + ([inhibitor]/IC_{50})c]$ to the data, where y is PfCRT^{Dd2}-mediated CQ transport, y_{min} and y_{max} are the minimum and maximum values of y, and c is a fitted constant. PfCRT^{Dd2}-mediated CQ transport was calculated by subtracting the uptake measured in oocytes expressing PfCRT^{D10} from that in oocytes expressing PfCRT^{Dd2}. Note that non-injected oocytes and oocytes expressing PfCRT^{D10} take up [³H]CQ to similar (low) levels via simple diffusion of the neutral species; this represents the 'background' level of CQ accumulation in oocytes (refer to [9] for full data and a detailed discussion).

The influx of unlabelled QC (10 or 40 μM) and MB (75 μM) was detected using the intrinsic fluorescence of these drugs and the uptake assays were performed at pH 6.0 and pH 5.0, respectively. The composition of the pH 5.0 ND96 buffer was 96 mM NaCl, 2 mM KCl, 1 mM MgCl$_2$, 1.8 mM CaCl$_2$, and 20 mM homo-PIPES. A subset of experiments attempted to measure the transport of unlabelled AO (75 or 150 μM) at pH 4.5, 5.0, 5.5, and 6.0. The fluorescence-based experiments were performed as described for the radioisotope uptake assays with the following modifications. At the completion of the incubation, the washed oocytes were transferred to separate wells of a flat 96-well plate (NUNC or PerkinElmer) that had been preloaded with 200 μL of 10% SDS. Each plate included a standard curve that consisted of 10 different concentrations of the fluorescent substrate under study, with each

sample being prepared in a 10% SDS solution containing a lysed oocyte (see Supplementary Figure 2). The plates were incubated overnight at room temperature and mixed on an orbital shaker the following day for approximately 5 minutes. The fluorescence intensity was measured using either a BMG Labtech FLUOstar Optima or a Tecan Infinite M1000 PRO plate-reader. The excitation and emission wavelengths were as follows: QC, 440 and 510 nm; AO, 485 and 520 nm; MB, 668 and 682 nm.

The kinetic parameters for QC and MB transport via PfCRT^{Dd2} (Figures 4D and 5D, respectively) were determined in SigmaPlot by a least-squares fit of the Michaelis-Menten equation ($v = V_{max}$[substrate]/(K_m + [substrate])) to the data.

In all cases, at least three independent experiments were performed (on different days and using oocytes from different frogs), and within each experiment measurements were made from 10-12 oocytes per treatment.

Supplementary Table 1. In Vitro Antiplasmodial Activity of Chloroquine (CQ) against 3D7 and K1 *P. falciparum* Parasites in the Absence or Presence of Acridine Orange (AO) or Verapamil (VP).

Strain[b]	IC$_{50}$ (nM)[a]		
	CQ	CQ + 250 nM AO	CQ + 1 µM VP
3D7	17 ± 4	14 ± 5	15 ± 4
K1	131 ± 11	93 ± 14[c]	46 ± 10[c]

Abbreviations: IC$_{50}$, half-maximal inhibitory concentration.

[a]The IC$_{50}$s are shown as the mean ± SEM from 3 independent experiments (performed on different days), within which measurements were averaged from 3 replicates.

[b]3D7 is a field-derived CQ-sensitive strain from Africa and K1 is a field-derived CQ-resistant strain from Thailand.

[c]A student *t*-test comparison with the CQ IC$_{50}$ determined for the K1 strain in the absence of AO or VP yielded a *P* value less than 0.05.

Supplementary Table 2. Percentages of Chloroquine, Quinacrine, and Acridine Orange in their Neutral, Monoprotonated (H⁺), or Diprotonated (H$_2^{2+}$) Forms in Solutions of Different pH.

pH	CQ			QC			AO[a]	
	% CQ	% CQH$^+$	% CQH$_2^{2+}$	% QC	% QCH$^+$	% QCH$_2^{2+}$	% AO	% AOH$^+$
5.0	0.0000005	0.0799997	99.9199998	0.0000005	0.1261314	99.8738681	0.0015849	99.9984151
5.5	0.0000050	0.2525445	99.7474505	0.0000050	0.3977775	99.6022175	0.0050116	99.9949884
6.0	0.0000497	0.7942781	99.2056722	0.0000495	1.2471555	98.7527951	0.0158464	99.9841536
6.4	0.0003100	1.9714568	98.0282332	0.0003065	3.0747290	96.9249645	0.0397949	99.9602051
6.9	0.0029731	5.9792417	94.0177852	0.0028739	9.1167741	90.8803520	0.1257343	99.8742657
7.4	0.0263210	16.7393496	83.2343294	0.0240013	24.0772048	75.8987939	0.3965286	99.6034714
8.4	1.0392882	66.0955322	32.8651795	0.7522247	75.4603423	23.7874330	3.8286504	96.1713496

The percentages were calculated using the Henderson-Hasselbach equation (pH = pK$_a$ + log ([A⁻] / [HA])) using the pK$_a$ values shown in Supplementary Figure 1.

Abbreviations: CQ, chloroquine; CQH$^+$, monoprotonated chloroquine; CQH$_2^{2+}$, diprotonated chloroquine; QC, quinacrine; QCH$^+$, monoprotonated quinacrine; QCH$_2^{2+}$, diprotonated quinacrine; AO, acridine orange; AOH$^+$, monoprotonated acridine orange.

[a]Note that the concentration of the neutral form of AO at pH 5.0 is 32-fold greater than that of neutral QC at pH 6.0.
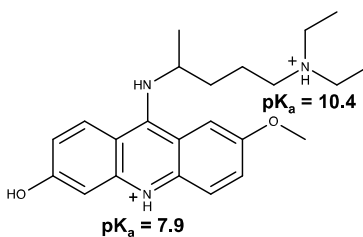
Supplementary Figure 1. The structures of the compounds used in this study. Abbreviation:

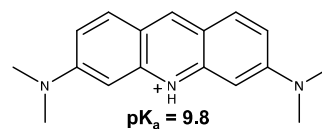pK$_a$, the negative logarithm to the base 10 of the acid dissociation constant (K$_a$).
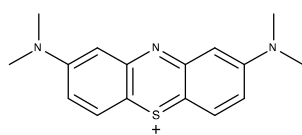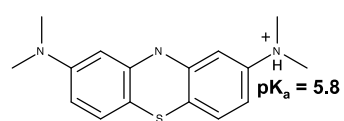
Chloroquine

pK$_a$ = 10.2

pK$_a$ = 8.1

Quinacrine

pK$_a$ = 10.4

pK$_a$ = 7.9

Acridine Orange

pK$_a$ = 9.8
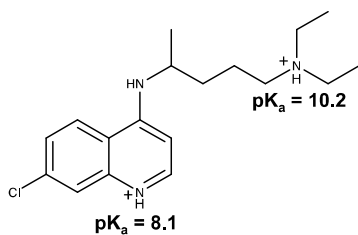
Methylene Blue
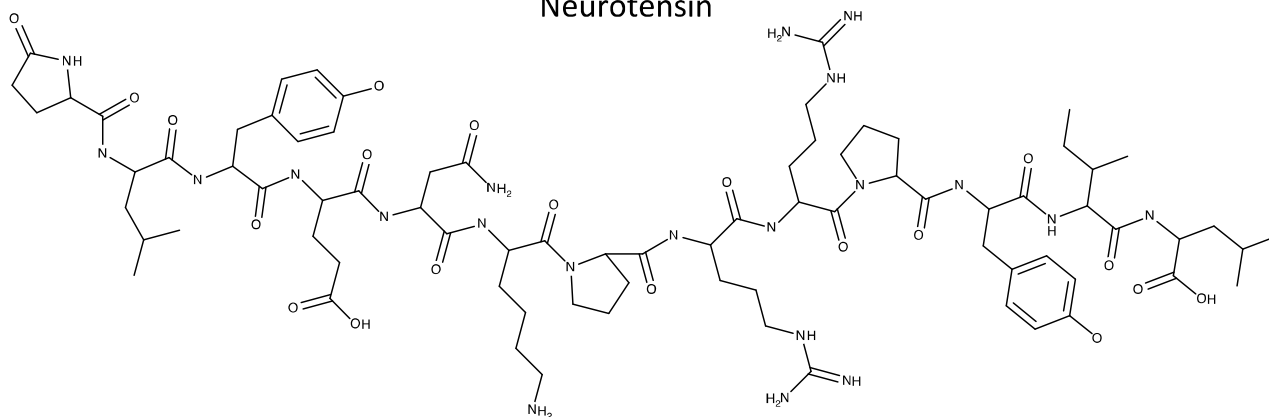
Leuco-Methylene Blue

pK$_a$ = 5.8

Saquinavir
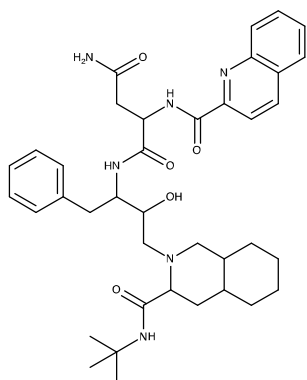
Verapamil
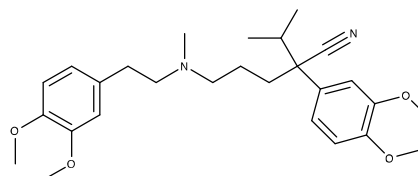
Neurotensin

Supplementary Figure 2. The fluorescence intensities of quinacrine (QC), acridine orange (AO), and methylene blue (MB) are linear with concentration in a 10% SDS solution containing a lysed oocyte. The drug influx assays entail dissolving each oocyte in 200 μL of a 10% SDS solution to release the accumulated drug. Given that the resulting oocyte debris could reduce the level of excitation energy that reaches the compound and/or absorb the emitted fluorescence, it was necessary to prepare each concentration standard in 200 μL of a 10% SDS solution that contained a lysed oocyte. *A*, The fluorescence intensity of QC, which was measured at an excitation wavelength of 440 nm and an emission wavelength of 510 nm, was linear with concentration between 0.001 and 1 μM. *B*, The fluorescence intensity of AO, which was measured at an excitation wavelength of 485 nm and an emission wavelength of 520 nm, was linear with concentration between 0.0625 and 2 μM. *C*, The fluorescence intensity of MB, which was measured at an excitation wavelength of 668 nm and an emission wavelength of 682 nm, was linear with concentration between 0.2 and 100 nM. The data represent the mean ± SEM from 3 to 11 independent experiments, performed on different days and using oocytes from different frogs. The error bars for each of the data points fell within the symbols.
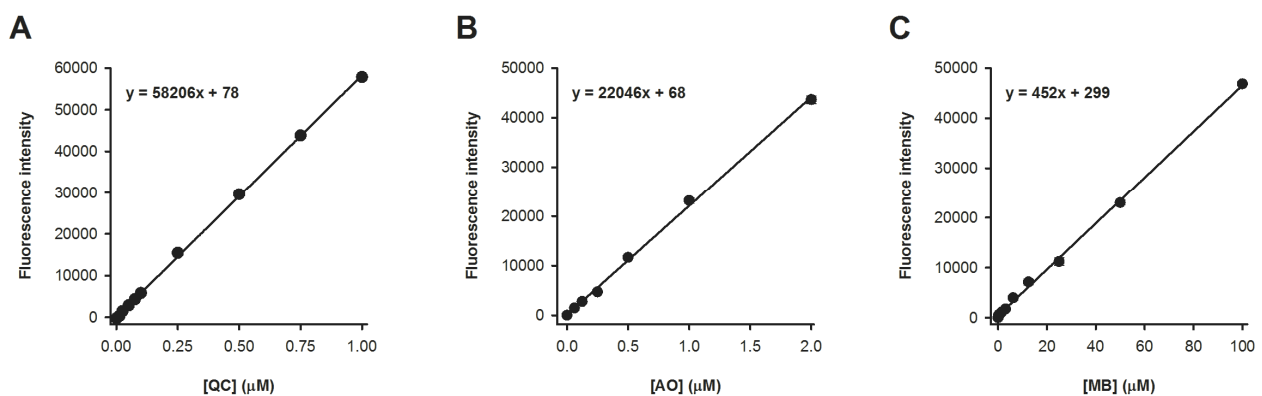
Supplementary Figure 3. The effect of chlorpheniramine (CP) on the accumulation of radiolabelled chloroquine ([³H]CQ) or radiolabelled acridine orange ([³H]AO) by erythrocytes infected with mature trophozoite-stage parasites. The white, black, and gray bars show data for the C2^{GCO3}, C4^{Dd2}, and C6^{7G8} parasite lines, respectively, under control conditions or in the presence of 2.5 μM CP. The accumulation of [³H]drug was expressed as a 'distribution ratio' (i.e., the concentration of [³H]drug within the infected cells relative to the concentration in the extracellular medium) and is shown relative to the ratio measured in the C2^{GCO3} parasites in the absence of CP. The data represent the mean + range/2 of 2 independent experiments (performed on different days), within which measurements were averaged from 2 replicates.
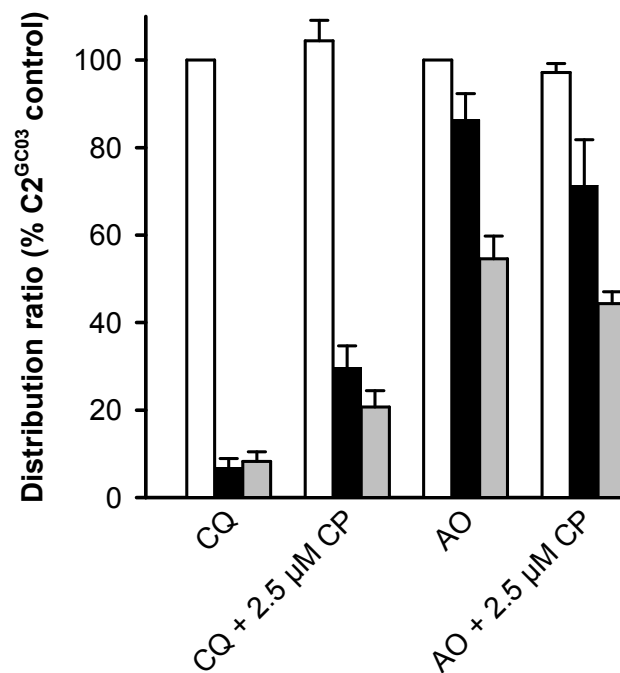
References

1. Desjardins, R.E., C.J. Canfield, J.D. Haynes, J.D. Chulay. Quantitative assessment of antimalarial activity in vitro by a semiautomated microdilution technique. Antimicrob Agents Chemother **1979**; 16:710-8.

2. Makler, M.T., J.M. Ries, J.A. Williams, et al. Parasite lactate dehydrogenase as an assay for *Plasmodium falciparum* drug sensitivity. Am J Trop Med Hyg **1993**; 48:739-41.

3. Fivelman, Q.L., I.S. Adagu, D.C. Warhurst. Modified fixed-ratio isobologram method for studying *in vitro* interactions between atovaquone and proguanil or dihydroartemisinin against drug-resistant strains of *Plasmodium falciparum*. Antimicrob Agents Chemother **2004**; 48:4097-102.

4. van Schalkwyk, D.A., W. Priebe, K.J. Saliba. The inhibitory effect of 2-halo derivatives of D-glucose on glycolysis and on the proliferation of the human malaria parasite *Plasmodium falciparum*. J Pharmacol Exp Ther **2008**; 327:511-7.

5. Odds, F.C. Synergy, antagonism, and what the chequerboard puts between them. J Antimicrob Chemother **2003**; 52:1.

6. Lehane, A.M., D.A. van Schalkwyk, S.G. Valderramos, D.A. Fidock, K. Kirk. Differential drug efflux or accumulation does not explain variation in the chloroquine response of *Plasmodium falciparum* strains expressing the same isoform of mutant PfCRT. Antimicrob Agents Chemother **2011**; 55:2310-8.

7. Saliba, K.J., H.A. Horner, K. Kirk. Transport and metabolism of the essential vitamin pantothenic acid in human erythrocytes infected with the malaria parasite *Plasmodium falciparum*. J Biol Chem **1998**; 273:10190-5.

8. Green, S.L. *The laboratory* Xenopus *sp.* M.A. Suckow ed. 1st ed. Boca Raton: CRC Press, **2010**:136-38.

9.   Martin, R.E., R.V. Marchetti, A.I. Cowan, S.M. Howitt, S. Bröer, K. Kirk. Chloroquine transport via the malaria parasite's chloroquine resistance transporter. Science **2009**; 325:1680-2.

10.   Hayward, R., K.J. Saliba, K. Kirk. The pH of the digestive vacuole of *Plasmodium falciparum* is not associated with chloroquine resistance. J Cell Sci **2006**; 119:1016-25.

11.   Klonis, N., O. Tan, K. Jackson, D. Goldberg, M. Klemba, L. Tilley. Evaluation of pH during cytostomal endocytosis and vacuolar catabolism of haemoglobin in *Plasmodium falciparum*. Biochem J **2007**; 407:343-54.

12.   Kuhn, Y., P. Rohrbach, M. Lanzer. Quantitative pH measurements in *Plasmodium falciparum*-infected erythrocytes using pHluorin. Cell Microbiol **2007**; 9:1004-13.

13.   Saliba, K.J., K. Kirk. pH regulation in the intracellular malaria parasite, *Plasmodium falciparum*. H^+ extrusion via a V-type H^+-ATPase. J Biol Chem **1999**; 274:33213-9.